Biogeosciences
Discussions

Reviews and syntheses: Systematic Earth observations for use in terrestrial carbon cycle data assimilation systems

Marko Scholze[1], Michael Buchwitz[2], Wouter Dorigo[3], Luis Guanter[4], and Shaun Quegan[5]

[1]Department of Physical Geography and Ecosystem Science, Lund University, Lund, Sweden
[2]Institute of Environmental Physics (IUP), University of Bremen, Bremen, Germany
[3]Department of Geodesy and Geoinformation, Vienna University of Technology (TU Wien), Vienna, Austria
[4]Remote Sensing Section, German Research Center for Geosciences (GFZ), 14473 Potsdam, Germany
[5]Centre for Terrestrial Carbon Dynamics, The University of Sheffield, Sheffield S3 7RH, U.K.

Correspondence to: M. Scholze (marko.scholze@nateko.lu.se)

Abstract.

The global carbon cycle is an important component of the Earth system and it interacts with the hydrological, energy and nutrient cycles as well as ecosystem dynamics. A better understanding of the global carbon cycle is required for improved projections of climate change including

5 corresponding changes in water and food resources and for the verification of measures to reduce anthropogenic greenhouse gas emissions. An improved understanding of the carbon cycle can be achieved by model-data fusion or data assimilation systems, which integrate observations relevant to the carbon cycle into coupled carbon, water, energy and nutrient models. Hence, the ingredients for such systems are a carbon cycle model, an algorithm for the assimilation, and systematic and

10 well error-characterized observations relevant to the carbon cycle. Relevant observations for assimilation include various in-situ measurements in the atmosphere (e.g. concentrations of CO_2 and other gases) and on land (e.g. fluxes of carbon water and energy, carbon stocks) as well as remote sensing observations (e.g. atmospheric composition, vegetation and surface properties).

We briefly review the different existing data assimilation techniques and contrast them to model

15 benchmarking and evaluation efforts (which also rely on observations). A common requirement for all assimilation techniques is a full description of the observational data properties. Uncertainty estimates of the observations are as important as the observations themselves because they similarly determine the outcome of such assimilation systems. Hence, this article reviews the requirements of data assimilation systems on observations and provides a non-exhaustive overview of current

20 observations and their uncertainties for use in terrestrial carbon cycle data assimilation. We report on progress since the review of model-data synthesis in terrestrial carbon observations by Raupach et al. (2005) emphasising the rapid advance in relevant space-based observations.

Biogeosciences

Discussions

Open Access

EGU

1 Introduction

The anthropogenic pertubation of the global carbon cycle has led to a global mean increase of 43%
in atmospheric CO_2 (from 280 ppm to 398 ppm) in 2014 compared to pre-industrial (before 1750)
levels (WMO, 2015), and is the main driver for climate change. The main causes for the increase in
CO_2 are burning of fossil fuels and land use change, which amount to emissions of 9.8 ± 0.5 GtC in
2014. However, only about 44% of these emissions stay in the atmosphere, the remainder is currently
taken up by the land biosphere ($\approx 30\%$) and the surface ocean ($\approx 26\%$) (Le Quéré et al., 2015). Pos-
itive climate-carbon cycle feedbacks, predominantly acting on land processes, may reduce this sink
capacity and thus accelerate global warming (Matthews et al., 2007). Also, the sink strength of the
terrestrial biosphere is more variable than that of the ocean (Ciais et al., 2013) and its quantification
by process-based terrestrial carbon cycle models exhibit large uncertainties (Le Quéré et al., 2015).

A common way to reduce uncertainties from process-based modelling is by confronting these
models with observational data. Raupach et al. (2005) pointed out that the systematic combination
of observational data with process modelling, which is commonly refered to as 'model-data fusion',
is an effective strategy for observing the Earth system. Model-data fusion, or more formally known
as data assimilation, is motivated by several benefits to make best use of observations and models
(Mathieu and O'Neill, 2008). These benefits include, among others, (1) forecasting and initialisation
(forward predictions in time based on past observations), (2) model and data quality control (regular
and systematic confrontation of model output with observations within their uncertainty statistics),
(3) combination of various data streams (combined constraints of independent observations can be
stronger than the sum of the individual constraints), (4) filling in regions with sparse observations
(consistent propagation of information from data-rich regions to data-poor regions), (5) estimating
unobservable quantities (through process-based relations in the model observations constrain mod-
elled quantities which are not directly measured) and (6) observing system design (what is the delta
of a new observation/instrument).

Systematic observations are a key ingredient for model-data fusion studies. Here, we focus on the
carbon cycle and the land-atmosphere system. The land-atmosphere components of the carbon cycle
are an important part of an integrated Earth observation system because of the close interactions on
land between the carbon cycle and the water and energy cycles, and hence its importance for climate
projections and climate change mitigation strategies through the monitoring and management of
terrestrial greenhouse gas sources and sinks.

Raupach et al. (2005) provide an analysis of the various elements of a Terrestrial Carbon Obser-
vation System (TCOS). The need, design and steps to be taken towards a TCOS were already out-
lined by others before (Cihlar et al., 2002; Global Carbon Project, 2003) but Raupach et al. (2005)
systematically reviewed two major components of a TCOS: the model-data fusion methods and
the observational data and data uncertainty characterisctics for some selected, main kinds of rele-
vant data. The requirements for a policy-relevant carbon observing system have been outlined by

60 Ciais et al. (2014). They review the current systematic carbon-cycle observations and illustrate the implementation of such a policy-relevant carbon observing system.

In this paper we provide an update of the observational data and data uncertainty characteristics as assessed by Raupach et al. (2005) with a focus on exisitng but also new and upcoming, relevant space-based observations (in the following referred to as Earth Observation (EO) data). In contrast

65 to Ciais et al. (2014), who focus on carbon-cycle observations, we focus here on any kind of relevant observational data to be (potentially) assimilated in a terrestrial carbon cycle data assimilation system (CCDAS). In a CCDAS the observations are used to constrain the underlying model (i.e. to move model output quantities closer to the observations and reduce their posterior uncertainties) usually by parameter optimisation. In that sense we are somewhat broader in terms of observed vari-

70 ables because also 'non-carbon' observations (such as soil moisture or land surface temperature) are able to constrain the carbon cycle indirectly through process information embedded in the underlying models. At the same time, the focus of our review is narrower than that of Ciais (2014), who also addressed ocean and anthropogenic components. Our focus lies on the terrestrial carbon cycle, because of the higher spatial and temporal variability in the net exchange fluxes and their associated

75 higher uncertainties than form the ocean and anthropogenic components.

The paper is organized as follows: in the next section we contrast data assimilation to recently established benchmarking activities and give a brief overview of commonly used data assimilation approaches and their applications in terrestrial carbon cycling. We continue with a short overview on data characteristics inlcuding an update on progress for some of the observations discussed in

80 Raupach et al. (2005). Since there has been much developments in the provision of remotely sensed observations we focus here on the characteristics of the most relevant EO data streams.

2   Model-data fusion

2.1   Data assimilation versus benchmarking

In the recent past the international land surface and terrestrial ecosystem modelling communi-

85 ties have recognized the importance of model benchmarking and evaluation (e.g. Luo et al., 2012; Foley et al., 2013). One of the reasons for this development is the huge range of model results from different models in key diagnostics of the land-atmosphere interface such as gross primary productivity (GPP) and latent heat flux (Prentice et al., 2015).

In general 'benchmarking' is understood as the quantification of performance against a reference

90 using some pre-defined metrics. The reference can either be output from some previous model simulations, other (ensembles of) models or reference datasets based on observations if the model simulates the analogue quantity. Luo et al. (2012) suggest a theoretical framework for benchmarking land models based on based on standardized references and metrics to measure model performance skills. A large variety of such metrics and their characteristics is introduced by Foley et al. (2013). Some

95　examples of benchmarking terrestrial carbon cycle models (either standalone or coupled to climate
models) are given by e.g. Randerson et al. (2009), Cadule et al. (2010) and Kelley et al. (2013).

The commonality between benchmarking/evaluation and data assimilation lies in the quantitative
assessment of model output. In benchmarking the quantitative assessment is performed by calculat-
ing some metrics against either observations or other references, while in data assimilation this is

100　achieved by defining a cost function, which quantifies the mismatch of some simulated model quan-
tity against observations weighted by their uncertainties (including a model uncertainty). But data
assimilation goes beyond benchmarking as it minimises the quantified mismatch to improve model
performance directly by adjusting either initial and boundary conditions, state variables and/or model
process parameters.

105　As pointed out by Prentice et al. (2015) there is a need for both model benchmarking and data
assimilation: Benchmarking as a routine application to improve confidence and evaluate the perfor-
mance (over time) in terrestrial carbon cycle modelling. However, if a benchmark test for a given
model fails this could simply imply that the model parameter values have not been specified correctly
and optmised against observations. In contrast, data assimilation, in particular when used for param-

110　eter optimisation, potentially identifies structural model and/or data deficiencies if the model-data
mismatch (or the benchmar test) is still inadequate after optimisation (see also Figure (1)).

2.2 Data assimilation methods

The general problem of model-data fusion, or, more strictly speaking, data assimilation can be for-
mulated like this: Given a model M, a set of observations $\mathbf{y}$ of some observables $\mathbf{o} = H(\mathbf{z})$, with

115　$\mathbf{z}$ being the state variables of the model and H the observation operator, and prior information on
some target variables $\mathbf{x}$, produce an updated description of $\mathbf{x}$. $\mathbf{x}$ may include elements of $\mathbf{z}$ and $\mathbf{p}$
(parameter, quantities not changed by the model, i.e. process parameters, boundary and initial condi-
tions). Here, we follow the notation as introduced by Rayner et al. (2016). The observation operator
maps the model state onto observables. In the case of a CCDAS assimilating atmospheric CO_2 the

120　observation operator is the atmospheric transport model mapping the net CO_2 surface exchange
fluxes as calculated by the terrestrial carbon cycle onto simulated atmospheric CO_2 concentrations.
In transport inversions the dynamical model, the atmospheric transport model, is also the observation
operator.

A data-assimilation system consists of three main ingredients: a set of observations, a dynamical

125　model including the observation operator and an assimilation method. In the Bayesian formulation
of the assimilation problem uncertainties (i.e. the description of quantities by probability density
functions, PDFs) are central to the concept of data assimilation. Both observations as well as models
have errors arising for various reasons. We will detail the observational errors in the next section.
Dynamical models as well as observation operators have errors arising from the parameterizations,

130 and the discretization of analytical dynamics into a numerical model; for a more complete description
of uncertainty in Earth System models or components of such we refer to Scholze et al. (2012).

We distinguish two basic approaches in data assimilation: sequential assimilation, which assim-
ilates observations at discrete time-steps and thus evolves over time according to the dynamical
model; and variational assimilation, which assimilates all observations at once at their respective

135 measyurement time over a given period, the so-called assimilation window. They differ in their nu-
merical efficiency and optimality for their specific use. A general data-assimilation scheme is shown
in Figure (1). In the sequential approach the inner loop is evaluated sequentially over time following
the dynamics of the model. In the case of variational assimilation the inner loop is evaluated itera-
tively (assuming a non-linear model) until a cost function minimum is found. The cost function is

140 formulated as

$$J = \frac{1}{2} \left[(\mathbf{x} - \mathbf{x}^{\mathrm{b}})^T \mathbf{B}^{-1} (\mathbf{x} - \mathbf{x}^{\mathrm{b}}) + (\mathrm{H}(\mathbf{x}) - \mathbf{y})^T \mathbf{R}^{-1} (\mathrm{H}(\mathbf{x}) - \mathbf{y}) \right],$$ (1)

where $\mathbf{x}^{\mathrm{b}}$ is the prior information, $\mathbf{B}$ the prior uncertainty covariance, and $\mathbf{R}$ the observational
uncertainty covariance. From Equation 1 follows that data and prior knowledge cannot be treated
separately from their respective uncertainties (Raupach et al., 2005). In other words, observations

145 (or prior knowlegde) for data assimilation are only complete if we know the full probability density
function (PDF), which, in the case of a Gaussian, can be characterised by its mean and variance. In
practical terms, the observational uncertainty covariances weight the model-data mismatch, while
the prior uncertainty covariances weight the deviation of the target variables from their prior values.
We note here that in the Gaussian case the model and observation operator errors can be added

150 quadratically to the observation errors.

An important diagnostic in data assimilation is the posterior uncertainty, which usually, because
of its high dimension, is hard to compute. If the assimilation problem is Gaussian the computation of
the posterior uncertainty covariance matrix simplifies and it can be approximated by the inverse of
the Hessian ($2_n d$ derivative) of the cost function. Typically, gradient-based optimisation approaches

155 approximate the Hessian, alternatively ensembles can be used to derive realisations of the poste-
rior PDF. The uncertainty reduction relative to the prior (i.e. $1 - \mathbf{U_{xpo}}/\mathbf{B}$ with $\mathbf{U_{xpo}}$ the posterior
uncertainty) then is a measure of the observational constraint on the target variables.

Rayner et al. (2016) introduce the theory fundamental to data assimilation and illustrate how the
different implementations of data assimilation relate to this theory in a more narrative style A more

160 complete and mathematically precise introduction to the concepts of data assimilation is given in the
textbooks by e.g. Daley (1991); Tarantola (2005).

2.3 Examples of terrestrial carbon cycle data assimilation

A variety of the methods as described by Rayner et al. (2016) have been applied by the carbon cy-
cle community. One example making use of formal assimilation methdologies for inferring surface-

165   atmosphere CO_2 exchange fluxes is based on atmospheric transport inversions. As mentioned before, in atmospheric inversions the observation model is an atmospheric tracer transport model. In atmospheric inversions both sequential and variational methods have been used together with observations of atmospheric trace gas concentrations such as from the flask sampling network, continuous in-situ and aircraft measurements and more recently also remotely sensed total column measurements. The

170   techniques for atmospheric transport inversions have been detailed in Enting (2002) and a recent comparison of results from different transport inversion is given by Peylin et al. (2013).

   A more recent development is the assimilation of observations into terrestrial biosphere models. Here, various methods and observations have been used to optimise model process parameters at different scales. A comparison of a whole suite of these assimilation methods applied to a test case

175   using a simplified model at local-scale is given by Trudinger et al. (2007) and Fox et al. (2009).

   Kaminski et al. (2002) were among the first who applied a formal algorithm together with observations of atmospheric CO_2 concentrations to constrain the Simple Diagnostic Biosphere Model at global scale. This work was continued by the development of the first Carbon Cycle Data Assimilation System with a process-based model at its core (Rayner et al., 2005). The advantage of using

180   a process-based model at the core of a CCDAS is that once the process parameters have been optimised the the constrained model can also be used for predictions as demonstrated by Scholze et al. (2007). Also, such systems are capable of ingesting multiple independent data streams besides atmospheric CO_2 concentrations. Kaminski et al. (2013) provide an overview on the developments of the CCDAS-BETHY since its first application while Scholze et al. (2016) demonstrate the latest ap-

185   plication of CCDAS-BETHY assimilating atmospheric CO_2 and remotely sensed surface soil moisture simultaneously. Since then several global terrestrial ecosystem models have been included in Carbon Cycle Data Assimilation Systems employing a variational approach (e.g. Schürmann et al., 2016; Peylin et al., 2016).

   Concurrently, there have been several studies at the local/regional scale assimilating various types

190   of observations. For instance, Barrett (2002) used a genetic algorithm to infer soil carbon turnover times in a terrestrial carbon cycle model over Australia from plant production, biomass, litter and soil carbon observations. Local eddy covariance flux tower measurements of net exchange of CO_2 and latent and sensible heat fluxes have been assimilated to optimize parameter related to photosynthesis, respiration and energy fluxes of terrestrial ecosystem models, using Monte Carlo type methods

195   (e.g. Braswell et al., 2005; Knorr and Kattge, 2005; Moore et al., 2008; Ricciuto et al., 2008), sequential methods (Williams et al., 2005), as well as variational approaches (e.g. Wang et al., 2001; Kuppel et al., 2012; Raoult et al., 2016)

   Recent advances are focusing on multiple independent data stream assimilation to provide a more rigorous constraint on the multiple components of terrestrial ecosystem models and avoid equifinal-

200   ity, i.e. different parameter solutions provide the same cost function value. Examples for such studies on local/regional scale are the assimilation of eddy covariance CO_2 fluxes together with observations

of vegetation structural information or carbon stocks (e.g. Richardson et al., 2010; Keenan et al., 2012) or together with remotely sensed vegetation activity such as the Fraction of Absorbed Photosynthetic Active Radiation (FAPAR) (e.g. Kato et al., 2013; Bacour et al., 2015). The assimilation

205 of multiple data streams can be performed either in a step-wise (e.g. Peylin et al., 2016) or simultaneous approach (e.g. Kaminski et al., 2012); in the case of non-linear models only the simultaneous assimilation makes optimal use of the observations (MacBean et al., 2016).

3   Data characteristics and provision

Observations are our measurable representation of the 'Truth'. They come with different charac-
210 teristics in terms of spatial and temporal resolution, coverage of the observed system, and errors. In analogy, models are also some representation of the 'Truth', however, via knowledge embodied in some form of functional relationships (with their own errors as mentioned before). The paper by Raupach et al. (2005) has been instrumental in highlighting the challenges in combining models and observational data for building a TCOS focussing on the observational requirements. Ciais et al.
215 (2014) argue for a globally integrated carbon observation system to improve our understanding of the carbon cycle for predicting future changes and to be able to independently verify the impact of emission reduction measures. Such a system relies on atmospheric carbon observations as a backbone but also concerns observations of the terrestrial and ocean carbon cycle. They focus on a strategy towards a global carbon-cycle monitoring system for achieving the above mentioned objectives.

220   Figure (2) depicts exemplarily the main observations of a TCOS and their space-time characteristics. In the following we briefly summarise the aspects of uncertainty in the observations and highlight progress on the specification of uncertainty for some of the observations in Fig. (2) as well as on their monitoring since Raupach et al. (2005).

3.1   Observational uncertainty

225 As mentioned before an important ingredient to any model-data fusion system are not only the observations themselves but also the uncertainties associated to them. We distinguish three main types of observation errors:

- Random: Random errors are always present in measurements and are caused by unpredictable changes in the measurement system (e.g. electronic noise in electrical instrument). They show
230   up as different readings of the same repeated measurement, and thus can be reduced by taking the average of multiple measurements. Random erros are usually assumed to be Normal (Gaussian) distributed, however, in some cases the random error distribution is log-normal (e.g. precipitation) or skewed by outliers due to unpredictable corruptions of the measurement system. Random erros are therefore relatad to the precision of a measurement system.

235   • Systematic (bias): Systematic errors in observations are usually due to some recurring prob-
             lems in the overall measurement system. They are caused by instrument miscalibrations or
             interferences with the measurement system. They can vary in space and time but they affect
             the measurement system in a predictable way. Biases can be both additive (absolute mean
             bias) and multiplicative (biases in the dynamic range affecting the amplitude of a signal). If
240   the source for systematic errors is known they can usually be fixed and shoud be removed.
             Systematic erros are therefore relatad to the accuracy of a measurement system.

          • Representativeness. The representation error occurs when information is represented at a scale
             different from the source of the information. For instance a quantity simulated by a model is
             'representative' for a given spatial and temporal resolution of the model grid. An individ-
245   ual measurement, however, represents information influenced by the local environment not
             resolved by the model grid (e.g. representation of atmospheric flask data in an atmospheric
             transport model gridcell). In the case of satellite-based observations the representation error
             also includes errors in inferring a biophysical quantity from the photons measured at the sen-
             sor. We come back to this issue later.

250   For both random and systematic errors not only the magnitude of the error for a single observation
     is important, i.e. the diagonal elements in the observational uncertainty covariance matrix $\mathbf{B}$, but also
     the correlations among errors for different observations. Hence there is a need to specify the off-
     diagonal elements in the error covariance matrix $\mathbf{B}$. These off-diagonal elements are usually hard to
     specify, however, they are important to quantify in a data assimilation system because they affect the
255 prediction of the optimal solution in the same way as the diagonall elements.

          As mentioned before, Raupach et al. (2005) have already reflected on the main properties of the
     data and their error covariances for observations of remotely sensed land surface properties (mainly
     NDVI), atmospheric CO_2 concentrations, land-atmosphere net CO_2 exchange fluxes, and terres-
     trial carbon stores. In the past years, there has been substantial progress in the specification of un-
260 certainties in eddy-covariance measurements of the land-atmosphere net CO_2 exchange flux (Net
     Ecosystem Productivity, NEP) and its component fluxes (GPP and ecosystem respiration, R_{eco}). For
     instance, Lasslop et al. (2008) analysed the error distribution and found that the eddy flux data can
     almost entirely be represented by a superposition of Gaussian distributions with inhomogeneous
     variance. In a more recent study Raj et al. (2016) investigated the uncertainy of GPP derived from
265 partitioning the eddy covariance NEP measurements. They used a light-use efficiency model em-
     bedded in a Bayesian framework to estimate the uncertainty in the separated GPP from the posterior
     distribution at half-hourly time steps. The availability of the eddy covariance data has also been
     heavily improved; the latest release of the FLUXNET2015 dataset now contains data from about
     165 sites worldwide spanning a period from 1991 (for some sites) up to 2014 (FLUXNET2015).

3.2 Towards operational carbon observation systems

In the European framework there have recently been major developments towards systematic in-situ observations for use in terrestrial carbon cycle data assimilation systems. The Integrated Carbon Observing System (ICOS) is a novel pan-European infrastructure for carbon observations, which will provide high-quality in-situ observations (both fluxes as well as atmospheric concentrations) over Europe and over ocean regions adjacent to Europe with a long-term perspective. ICOS consists of central facilities for co-ordination, calibration and data in conjunction with networks of atmospheric, oceanic and ecosystem observations as well as a data distribution centre, the Carbon Portal, providing discovery of and access to ICOS data products such as derived flux information. The ICOS network runs in an operational mode, and greenhouse gas concentrations and fluxes will be determined on a routine basis. The measurements are designed to allow up to daily determination of (mainly natural) sources and sinks at scales down to approximately 50 x 50 km^2 for the European continent.

An example for an operationalised, space-based Earth observing programme is the fleet of so-called Sentinel satellites of the European Copernicus programme. Copernicus aims at providing Europe with a continuous and independent access to Earth observation data and associated services (transforming the satellite and additional in-situ data into value-added information by processing and analysing the data) in support of Earth System Science (Berger et al., 2012). So far, six different Sentinel missions are planned out of which three are in operation and the remainder is scheduled to be launched during the next years. Each type of the currently foreseen Sentinels has a specific objective and will deliver a range of EO products. Some of these products will be suitable for constraining the terrestrial carbon cycle, such as soil moisture (Sentinel 1), FAPAR, leaf chlorophyl and water content and land cover (Sentinel 2 and 3), land surface temperature (Sentinel 3), atmospheric methane and flourescence (Sentinel 5 and precursor). So far, a dedicated mission for monitoring the carbon cycle, i.e. an instrument measuring the atmospheric CO_2 composition, is not yet included in the Copernicus monitoring programme (see Ciais et al., 2015), however, the series of Sentinel satellites is likely to be extended in the future.

3.3 Examples of systematic observations from satellite EO data

There has been a vast extension of EO capabilites during the past 10 years or so both in terms of product quality (including, for instance, improved accuracy) but also quantity (new products).

In any data assimilation system using satellite EO data one needs to decide in the design phase of the system whether to assimilate observations at the sensor level (i.e. the spectral radiances for optical sensors or brightness temperatures for microwave sensor, referred to as level 1 data) or to assimilate the bio-geophysical variable derived from the radiances through a retrieval algorithm (level 2 data product). When assimilating level 1 data the retrieval algorithm is part of the observation operator linking the model state to the observations in the data assimilation system. A more detailed

Biogeosciences
Discussions

305   description of the two alternatives in assimilating EO satellite observations into models of the Earth system is given by Kaminski and Mathieu (2016). In carbon cycle data assimilation systems level 2 data products (or even level 3 data, which are provided on a regular space-time grid) are most commonly used.

In the next subsections we present some selected, and for terrestrial carbon cycle data assimi-
310   lation most relevant remotely sensed Earth Observation products in more detail. The EO products described below (atmospheric CO_2, vegetation activity, soil moisture, terrestriaial biomass) either have already been used, are in the process of being used, or would potentially be a useful data constraint in a CCDAS. For vegetation activity we distinguish two major types of products: more 'traditional' reflectance- or radiative-based products such as fraction of absorbed photosynthetically
315   active radiation (FAPAR) and recently developed products based on biogeochamical processes such as sun-induced flourescence (SIF). For instance, FAPAR has already been demonstrated to provide a strong constraint on terrestrial carbon as well as water fluxes through its impact on the phenology components of the carbon cycle model (e.g. Knorr et al., 2010; Kaminski et al., 2012). SIF is a promising observation to constrain the gross uptake of CO_2 by plant photosynthesis. First assimi-
320   lation results using SIF observations in a CCDAS show that the uncertainty in global annual GPP is largely reduced by constraining parameters that describe leaf phenology (Norton et al., 2016). Also assimilation of XCO2 into a diagnostic terrestial carbon cycle model has been shown to derive net CO_2 fluxes consistent with independent in-situ measurements of atmospheric CO_2 as well as to reduce posterior uncertainties in the infered net and gross CO_2 fluxes (Kaminski et al., 2016b).
325   van der Molen et al. (2016) assessed the impact of assimilating various remotely sensed soil moisture products into the SiBCASA ecosystem model on simulated carbon fluxes in Boreal Eurasia. Although the impact of assimilating ASCAT surface soil moisture was significant, its skill in this hydrologically complex environment strongly depends on surface water and vegetation dynamics. In contrast, Scholze et al. (2016) showed that when assimilating SMOS soil moisture simultaneously
330   with in-situ atmospheric CO_2 concentrations the reduction of uncertainty in gross and net CO_2 fluxes relative to the prior is considerably higher than for assimilating CO_2 only, which quantifies the added value of SMOS observations as a constraint on the terrestrial carbon cycle. So far, remotely sensed biomass data have not been used in carbon cycle data assimilation studies, however, Thum et al. (2016) demonstrated the added value of in-situ observations of biomass increment in reducing un-
335   certainties in simulated above ground biomass mainly through the calibration of parameters in the carbon allocation scheme of the terrestrial carbon cycle model.

This list of EO products described in this paper is admittedly subjective and there is of course a whole range of additional remotely sensed products available, which are relevant for carbon cycle studies as well, e.g. burned area (e.g. Giglio et al., 2013), land cover (e.g. Bontemps et al., 2012),
340   land surface temperature (e.g. Li et al., 2013), leaf area index (which is in effect closely related to FAPAR) (e.g. Liu et al., 2014) or vegetation optical depth (e.g. Konings et al., 2016). However, these

products are rather used as input or boundary conditions for terrestrial carbon cycle models or, for instance in the case of vegetation optical depth, they have so far not been used in carbon cycle data assimilation studies.

3.3.1 Atmospheric CO_2 and CH_4

345

Satellite retrievals of atmospheric carbon dioxide (CO_2) and methane (CH_4) are available from several satellite instruments such as mid-tropospheric CO_2 and CH_4 columns from Infrared Atmospheric Sounding Interferometer (IASI) (e.g. Crevoisier et al., 2009a, b) on EUMETSAT's Metop satellite series, vertical profiles with highest sensitivity in the mid/upper troposphere from AIRS

350 on Aqua (e.g. Xiong et al., 2013), stratospheric profiles from MIPAS on ENVISAT limb observations (e.g. Laeng et al., 2015) and from the solar occultation observations of SCIAMACHY on ENVISAT (Noël et al., 2011, 2016) and ACE-FTS (e.g. Boone et al., 2005; Foucher et al., 2009). These observations have however only little or no sensitivity to CO_2 and CH_4 concentration changes close to the Earth's surface and therefore contain only limited information on regional or local

355 CO_2 and CH_4 sources and sinks. Satellites with high near-surface sensitivity are nadir (downlooking) satellites which measure radiance spectra of reflected solar radiation in the relevant spectral bands in the near-infrared/shortwave-infrared (NIR/SWIR) spectral region, which are located around 1.6 μm (CO_2 and CH_4) and around 2.0 μm (CO_2). Satellites instruments which perform (or have performed) these observations are SCIAMACHY onboard ENVISAT (2002–2012) (Burrows et al.,

360 1995; Bovensmann et al., 1999), TANSO-FTS onboard GOSAT (launched in 2009) (Kuze et al., 2009, 2014) and NASA's Orbiting Carbon Observatory 2 (OCO-2) mission (launched in 2014) (Crisp et al., 2004; Boesch et al., 2011).

The main CO_2 and CH_4 data products of these sensors are near-surface-sensitive column-averaged dry-air mole fractions of CO_2 and CH_4, denoted XCO2 and XCH4. The quantities XCO2 and XCH4

365 are both retrieved from SCIAMACHY/ENVISAT (ground pixel size: 30×50 km^2 (along track times across track); swath width 960 km with contiguous ground pixels) and TANSO-FTS/GOSAT (10 km pixel size; several (e.g. 3 or 5) non-contiguous pixels across track). OCO-2 delivers XCO2 (8 ground pixels across track, each $\approx$1.3 km) and in the near future other satellites will be launched such as Europe's Sentinel-5-Precursor satellite (S5P) (Veefkind et al., 2012), which will deliver (among

370 several other parameters) XCH4 (7 km pixel size at nadir, 2600 km swath width with contiguous ground pixels; planned launch: mid 2017) (Butz et al., 2012) and China's TanSat (planned launch end of 2016), which will deliver XCO2 with similar characteristics as NASA's OCO-2. In the following we will focus the discussion on sensors who have already delivered multi-year XCO2 and XCH4 year data sets, i.e. on SCIAMACHY and TANSO.

375 The XCO2 and XCH4 data products retrieved from SCIAMACHY and TANSO are generated from the radiance observations using different approaches. Most approaches are based on 'Optimal Estimation' (OE) (e.g. Rogers, 2000; Reuter et al., 2010), also called Bayesian inference.

OE permits to constrain the retrieval using a priori information on, e.g. atmospheric vertical profiles of trace gases and aerosols. In general, the radiances are simulated using a radiative transfer model (RTM) and RTM and other parameters (state vector elements) are adjusted until an 'optimal' match is achieved between observed and simulated radiances. One algorithm (WFM-DOAS (WFMD) (Buchwitz et al., 2000; Schneising et al., 2008, 2009)) is based on least-squares and does not use a priori information to constrain the fit parameters. As a consequence, the resulting XCO2 and XCH4 products are typically somewhat 'noisier' compared to the OE products.

The XCO2 and XCH4 data products from SCIAMACHY are generated within the GHG-CCI project (Buchwitz et al., 2015) of ESA's Climate Change Initiative (CCI, Hollmann et al. (2013)) and these products are available from the GHG-CCI website (http://www.esa-ghg-cci.org/). XCO2 and/or XCH4 products from GOSAT are generated at several institutions in Japan, Europe and the USA and are available from several sources as shown in Table (1). The quality of these GHG-CCI products and the XCO2 and XCH4 products generated elsewhere has been significantly improved during recent years (e.g. Schneising et al., 2012; Yoshida et al., 2013; Dils et al., 2014; Buchwitz et al., 2015) and has now reached quite high maturity when compared to user requirements as formulated in, e.g. GCOS (2011). This can be concluded, for example, from the quality of the latest version of the GHG-CCI SCIAMACHY and TANSO XCO2 and XCH4 data set ('Climate Research Data Package No. 3', CRDP3) (Buchwitz et al., 2016). Based on comparisons with ground-based observations of the Total Carbon Column Observing Network (TCCON, Wunch et al. (2010, 2011)) it has been found that the GCOS requirements for systematic error (< 1 ppm for XCO2, < 10 ppb for XCH4) and long-term stability (< 0.2 ppm/year for XCO2, < 2 ppb/year for XCH4) are met for nearly all products. As also shown in Buchwitz et al. (2016), the single observation (ground pixel) retrieval precision) random error primarily due to instrument noise) is about 2 ppm for XCO2 from SCIAMACHY and TANSO and $\approx$15 ppb for TANSO XCH4. For SCIAMACHY XCH4 the precision depends on time period and retrieval algorithm and is in the range 35 - 80 ppb. For some products it has also been investigated to what extent the uncertainty can be reduced upon averaging (Kulawik et al., 2016) and recommendations are given how to take into account error correlations (Reuter et al., 2016), i.e. which values to use for the non-diagonal elements of the error covariance matrix, as an important contrbution to the full characterisation of the data needs for data assimilaton studies.

Figure (3) presents an overview about GHG-CCI CRDP3 XCO2 (left) and XCH4 (right) data set in terms of time series and maps. These figures have been generated by gridding the underlying individual ground pixel (Level 2) products to generate a 5°×5° monthly Level 3 'Obs4MIPs' product Buchwitz and Reuter (2016). Each 5°×5° monthly grid cell also contains an estimate of the overall uncertainty (also shown in Fig. (3)) which has been computed taking into account random and systematic error components. As can be seen from Fig. (3), the uncertainty of the satellite XCO2 retrievals for monthly 5°×5° averages is estimated to be typically around 0.5 - 1 ppm (values larger

415   than 1 ppm are typically associated with regions where only few observations per grid cell exist,
      e.g. due to clouds or higher latitudes corresponding to low sun elevation). For XCH4 the uncertainty
      is on the order of a few ppb (typically 4 - 8 ppb). In Buchwitz and Reuter (2016), also initial TCCON
      validation results of the Obs4MIPs products are presented. It is shown that the XCO2 product agrees
      with monthly averaged TCCON XCO2 within 0.29 ± 1.2 ppm ($1\,\sigma$) and the XCH4 product within
420   2.0 ± 10.7 ppb. This is hardly worse that the results which have been obtained by careful valida-
      tion of the individual ground pixel retrievals taking into account the best possible spatio-temporal
      co-location and considering the averaging kernels, etc. (e.g. Buchwitz et al., 2016). Note that the
      computed differences of Obs4MIPs monthly $5°\times5°$ satellite products with monthly averaged TC-
      CON include the errors of the satellite data, errors of the TCCON products, errors due to neglecting
425   altitude sensitivity differences (averaging kernels), and representativity error. This indicates that the
      representativity error is quite small (at least for monthly $5°\times5°$ spatio-temporal sampling and res-
      olution), probably on the order of 0.1 - 0.2 ppm for XCO2 and a few ppb for XCH4 (it is planned
      to quantify this error in the future but currently only these rough estimates are available). Note that
      detailed information on all GHG-CCI products is available on the GHG-CCI website in terms of
430   technical documents, links to peer-reviewed publications and figures including detailed maps for
      each month and each individual data product.

      The SCIAMACHY and TANSO XCO2 and XCH4 retrievals have been used in a number of scien-
      tific studies to address important questions related to the sources and sinks of atmospheric CO_2 and
      CH_4 by atmospheric inversion studies (e.g. Bergamaschi et al., 2013; Houweling et al., 2015) and
435   more recently also in a data assimilation context for optimising model parameters (Chevallier et al.,
      2016). Obviously, the longer the time series and the more accurate it is, the larger the information
      content of a given data set. Therefore, further improvements are desired (Chevallier et al., 2016) and
      possible (at least in terms of time series extension but likely also in further reduction of remaining
      biases).

440   **3.3.2   Reflectamce-based vegetation dynamics/activity**

      Since the early beginnings of remote sensing the state and evolution of the vegetation has been
      monitored by satellites. An early attempt to analyse vegetation dynamics from space is to calculate
      the Normalized Difference Vegetation Index (NDVI, defined as the ratio between the difference of
      near-infrared, NIR, and visible red, Red, spectral bands and the sum of NIR and Red: NDVI = (NIR
445   - Red)/(NIR + Red), Deering et al. (1975)). The advantage of an index such as NDVI lies in its
      simplicity and applicability to sensors with few spectral bands such as the Advanced Very High Res-
      olution Radiometer (AVHRR). Therefore this index has been applied for numerous purposes over
      the last 30 years or so. But NDVI is not a geophysical variable and it is sensitive to various perturb-
      ing factors such as atmospheric constituents (aerosols, water vapor), directional effects (geometry
450   of illumination and observation), changes in soil background color changes (depending on soil wa-

ter content)(e.g. Pinty et al., 1993; Goel and Qin, 1994; Leprieur et al., 1994; Dorigo et al., 2007).
There have been many attempts in modifying NDVI and developing additional vegetation indices to
overcome its limitations, for example: Soil-Adjusted Vegetation Index (Huete, 1988), Atmospheri-
cally Resistant Vegetation Index (Kaufman and Tanre, 1992) or Global Environmental Monitoring
455 Index (Pinty and Verstraete, 1992). These indices generally exhibit some improvement in one respect
but at the expense of some degradation in another respect.

A rational approach to address all these issues at once is to design a physically based quantity
which closely follows the state of the vegetation. The Fraction of Absorbed Photosynthetically Ac-
tive Radiation (FAPAR) provides some kind of information on the photosynthetic activity of the
460 land vegetation. FAPAR is recognised as an Essential Climate Variable (ECV) (GCOS, 2011) and is
based on the land surface radiation budget. It is defined as the fraction of the photosynthetically active
radiation (i.e. incoming solar radiation in the spectral region 0.4–0.7μm) that is absorbed by the veg-
etation canopy (see also Pickett-Heaps et al. (2014) for a mathematical definition). Several FAPAR
products are derived from a variety of optical sensors (e.g. ATSR, MERIS, MISR, MODIS, SEVIRI,
465 SeaWiFS, VEGETATION) at different spatial and temporal resolutions. Although there has been
substantial efforts to harmonize products across sensors (Ceccherini et al., 2013) and establish stan-
dards and validation practices (e.g. Widlowski, 2010) there are still considerable differences among
the products. These differences can mainly be associated to differences in the retrieval methodology
as well as to the quality of input variables. A recent overview of various FAPAR products and their
470 specifications, but without an assessemt of product uncertainties, is given by Gobron and Verstraete
(2009). Table (2) summarises the characteristics of the most common FAPAR products.

Several studies have compared the performance of different satellite-derived FAPAR products:
McCallum et al. (2010) looked at four FAPAR datasets over Northern Eurasia for the year 2000,
Pickett-Heaps et al. (2014) evaluated six products across Australia, D'Odorico et al. (2014) com-
475 pared three products over Europe and Tao et al. (2015) assessed five products over different land
cover types. Pickett-Heaps et al. (2014) concluded that although all six evaluated products display
robust spatial and temporal patterns there is considerable disagreement amongst the products and
non of the products outperforms the others. One of the reasons for these differences are differ-
ent assumptions on the underlying biome types. They also reviewed the consistency of the FAPAR
480 products against in-situ field measurements, the mean difference between the EO products and the
in-situ field measurements is around 0.1 (as FAPAR is a normalised fraction values range from 0 to
1). This estimate is confirmed by the study of Tao et al. (2015) who suggest an average uncertainty
of 0.14 from validation against total FAPAR and 0.09 from validation against green FAPAR in-situ
measurements. In their comparison of Joint Research Centre–Two-stream Inversion Package (JRC-
485 TIP) MODIS, JRC MGVI and Boston University MODIS products (see Tab. 2) D'Odorico et al.
(2014) placed special emphasis on the assessment of the product uncertainties by not only compar-
ing the uncertainties (or quality indicators) as proposed by the product teams but also by calculating

an independent theoretical uncertainty based on the triple collocation (TC) method (see Sec. 3.3.4).
While the uncertainties specified by the product teams differed by up to 0.1 among the products, the

490   TC method suggested more consistent uncertainties among the three products of around 10-20% of
the signal.

The JRC-TIP (Pinty et al., 2007) is an inverse modelling system that was deliberately designed
to retrieve a set of land surface variables, including FAPAR, in a form that is compliant with the
requirements for assimilation into terrestrial biosphere models. TIP is based on a one-dimensional

495   two-stream representation of the radiative transfer in the canopy-soil system (Pinty et al., 2006) and
applies the same inversion approach as CCDAS, which is briefly sketched in 2.2 and detailed in
Rayner et al. (2016); Kaminski and Mathieu (2016). In a first step it retrieves a set of model param-
eters describing the state of the vegetation canopy system including their full uncertainty covariance
by combining prior information with observed radiant fluxes. Further, the model is used to propagate

500   this PDF forward onto the simulated fluxes such as FAPAR. TIP uses observed broadband albedo
in the NIR and visible spectral domains as input from which it retrieves the effective (i.e. model-
dependent) quantities such as FAPAR, leaf area index (LAI) besides other radiatitve quantities.
Long-term global records of JRC-TIP products (see 2) have been retrieved from broadband albe-
dos provided by MODIS collection 5 (Pinty et al., 2011b, c) and Globalbedo (Disney et al., 2016).

505   Products are provided for each of the respective 16-day (MODIS) and 8-day (Globalbedo) synthesis
periods. Both JRC-TIP records are provided in the native 1 km resolution of the albedo input prod-
ucts. In order to maintain the above-mentioned compliance with terrestrial models, coarser resolu-
tion products are to be derived by applying JRC-TIP to aggregated albedo inputs (as in Disney et al.,
2016). JRC-TIP products are validated at site (Pinty et al., 2007, 2008, 2011a) and regional scales

510   (Disney et al., 2016); more details on JRC-TIP are given in Kaminski et al. (2016a).

3.3.3   Biogeochemical-based vegetation activity

Sun-induced fluorescence (SIF) is an electromagnetic signal emitted as a two-peak spectrum be-
tween 650 and 850 nm by the chlorophyll$-a$ of green plants under solar radiation. SIF can be di-
rectly related to photosynthetic electron transport rates and yields a mechanistic link to photosyn-

515   thesis and the subsequent gross carbon uptake by terrestrial vegetation (GPP) (Porcar-Castell et al.,
2014). Recent developments in satellite-based spectroscopy have enabled the first retrievals of SIF
from space (Frankenberg et al., 2011c; Joiner et al., 2011), which holds the promise of enabling new
approaches to globally monitoring terrestrial photosynthesis. For example, a high linear correlation
between data-driven GPP estimates and SIF retrievals at global and annual scales was reported by

520   Frankenberg et al. (2011c); Guanter et al. (2012). The skills of SIF as a proxy for photosynthetic ac-
tivity and GPP were also reported by studies over different ecosystems, like the Amazon rainforest
(Lee et al., 2013; Parazoo et al., 2013), large crop belts (Guanter et al., 2014), and the boreal forests
in Eurasia and North America (Walther et al., 2015).

The global retrieval of SIF from space lies on the principle of *in-filling* of solar Fraunhofer lines
by SIF (Frankenberg et al., 2011b). Fraunhofer lines are absorption features in the solar spectrum,
caused by elements in the solar atmosphere and sufficiently resolved by atmospheric spectrometers.
Because of the additive nature of SIF, the fractional depth of the Fraunhofer lines detected by the
satellite instrument decreases with the amount of SIF being emitted at the same wavelength. The
retrieval of SIF from space is then based on the evaluation of the depth of the Fraunhofer lines
present in red and NIR top-of-atmosphere spectra. The retrieval forward model is thus simple and
can be linearised (e.g. Guanter et al., 2012; Köhler et al., 2015b), so the inversion can be easily
solved by least squares optimisation.

Fraunhofer line-based SIF retrievals tend to be accurate but not precise: uncertainties are domi-
nated by a random component associated to instrumental noise, which is linearly mapped into SIF
retrievals. The amplitude of instrumental noise, and hence 1-σ single-retrieval errors, scale with
at-sensor radiance for the most common case of grating-based spectrometers dominated by multi-
plicative noise. This implies that retrieval errors are mostly driven by surface brightness and sun
zenith angles (Guanter et al., 2015). Because of this high contribution of random errors to the to-
tal retrieval uncertainty, single SIF retrievals are commonly linearly-aggregated as spatio-temporal
composites in which random errors are reduced. The amount of retrievals to be aggregated into a
given gridbox results from a compromise between spatial resolution, temporal resolution and preci-
sion of the gridded product. The random uncertainty of the resulting spatio-temporal composites is
then not only driven by surface albedo and illumination, but also by the number of soundings going
into a given gridbox, which is in turn defined by cloudiness and latitude (in the case of overlapping
orbits). Detailed analyses of random errors in SIF retrievals for different spaceborne instruments can
be found in Frankenberg et al. (2011b) and Guanter et al. (2015).

Global SIF data sets have been or are being derived from GOSAT, MetOp's Global Ozone Mon-
itoring Experiment-2 (GOME-2), ENVISAT's SCIAMACHY and the OCO-2 mission (Joiner et al.,
2011; Frankenberg et al., 2011c; Guanter et al., 2012; Joiner et al., 2012, 2013; Köhler et al., 2015a,
b; Wolanin et al., 2015; Joiner et al., 2016; Frankenberg et al., 2014). Sample SIF maps from GOSAT,
GOME-2 and SCIAMACHY for July 2010 are displayed in Fig. 4. All four missions except for
SCIAMACHY are still operating. The spectal, spatial and temporal sampling of single SIF sound-
ings varies for each instrument, as it is summarised in Table 3. For example, GOME-2 and SCIA-
MACHY provide SIF retrievals in the red and NIR spectral regions with global coverage and a
relatively high temporal resolution. However, this comes at the expense of a coarse spatial resolu-
tion, which is $40 \times 80 \, \text{km}^2$ for GOME-2 ($40 \times 40 \, \text{km}^2$ for GOME-2 on MetOp-A since July 2013) and
$30 \times 240 \, \text{km}^2$ for SCIAMACHY. On the other hand, GOSAT and OCO-2 do not provide spatially-
continuous measurements (i.e. no global coverage), but single soundings in the NIR have a much
higher spatial resolution than those of GOME-2 and SCIAMACHY. In particular, OCO-2 soundings
correspond to ground areas of about $4 \, \text{km}^2$, which is substantially finer than that of the other data

Biogeosciences Open Access

Discussions

EGU

sets. The number of soundings per day by OCO-2 is also much larger (about 100x) than that by the other instruments (Frankenberg et al., 2014), which makes OCO-2 SIF to be the most suited data set for studies over areas not requiring a continuous spatial sampling but benefiting from a high spatial resolution. This is the case, for example, of tropical and boreal forests: spatial continuity is less criti-

565 cal for those ecosystems because they are relatively homogeneous over large spatial scales, whereas the high spatial resolution is important to maximise the number of clear-sky soundings during the parts of the year with persistent cloudiness.

Concerning near-future perspectives for SIF monitoring, it can be expected that the limitations in spatial resolution and coverage of existing SIF products will be alleviated with the advent of the

570 TROPOspheric Monitoring Instrument (TROPOMI) scheduled for launch onboard the Sentinel-5 Precursor satellite mission by mid 2017 (Table 3). TROPOMI will enable SIF retrievals in the red and NIR regions similar to GOME-2 and SCIAMACHY, but with a 7 km pixel, daily global coverage and a number of clear-sky observations per day $\approx$200 larger than GOME-2 and $\approx$600 larger than SCIAMACHY. The SIF product from TROPOMI can therefore be anticipated to have a much higher

575 spatio-temporal resolution and signal-to-noise ratio than those from GOME-2 and SCIAMACHY (Guanter et al., 2015). Complementary, the FLuorescence EXplorer (FLEX) (Drusch and FLEX Team, 2015) has recently been selected for implementation by ESA, with launch currently expected for 2022. FLEX will provide global measurements of SIF in the red and NIR with at a relatively low temporal resolution, but with the finest spatial resolution of all existing and upcoming spaceborne

580 instruments.

3.3.4 Soil moisture

Soil moisture is measured in-situ through large-scale soil moisture monitoring networks (Dorigo et al., 2011; Ochsner et al., 2013) or at various FLUXNET sites (Baldocchi et al., 2001). Yet, these point observations have only limited coverage in space time, have spatially very divergent properties

585 (Dorigo et al., 2013), and often contain large representativeness errors at the scale of global ecosystem models (Gruber et al., 2013). Satellite remote sensing in the microwave domain has the potential to overcome many of these issues. Microwave remote sensing uses the contrasting dielectric properties of water, air, ice, and soil particles to infer the water content in the soil column (Owe et al., 2008). Both passive radiometer systems, measuring the emitted microwave radiance ('brightness

590 temperatures'), and active radar systems, measuring backscattered microwave radiance, can be used to retrieve soil moisture. Microwave sensors operate in different frequency (wavelength) domains, of which L-band (with a wavelength of $\approx$23 cm) and C-band ($\approx$5 cm) are most commonly used for retrieving soil moisture (Kerr et al., 2012; Owe et al., 2008; Wagner et al., 1999). Smaller wavelengths are more sensitive to the vegetation canopy covering the soil and increasingly lose their sensitivity

595 to water. Still, frequencies up to 19 GHz ($\approx$1.5 cm) have proven potential for providing robust soil moisture estimates at the global scale for moderately to sparsely vegetated areas (Owe et al., 2008).

Biogeosciences
Discussions

Open Access

EGU

Due to the relatively low energy levels and the technical challenges in microwave domain, spatial resolutions of the satellite observations are generally coarse ($\approx$25–50 km) but with high revisit frequencies (up to 1 day). Only Synthetic Aperture Radar is able to provide much higher spatial resolutions up till a few meters, yet at the cost of the revisit times.

Since the release of the first global soil moisture datasets from microwave sensors in the early 2000s the number of available soil moisture products and missions has rapidly expanded (De Jeu and Dorigo, 2016). Several (pre-)operational products are now available from a wide variety of data providers and space organizations (Table 4). While initially soil moisture products were based on sensors mainly designed for other purposes (such as ASCAT, AMSR2, and Sentinel-1), ESA and NASA launched their own dedicated soil moisture satellite missions SMOS and SMAP (Kerr et al., 2012; Entekhabi et al., 2010). Apart from the Sentinel-1 mission, which primarily targets the provision of high resolution observations over Europe, all currently active missions provide a nearly global coverage at a coarse resolution approximately every 1-2 days. Differences between the various products exist in their technical design, observation bands, and retrieval algorithms, which often result in complementary strengths over different land cover types (Alyaari et al., 2015; Dorigo et al., 2010; Liu et al., 2011). The missions also differ in their degree of operationalization: While SMOS and SMAP are primarily scientific concept demonstrators, AMSR2 continues the legacy of C-band radiometer observations started by JAXA and NASA in 2002 with the launch of AMSR-E, while ASCAT is embedded in a fully operational program of weather observing satellites with a guaranteed continuation at least until 2023 and a follow-on mission already under development (Wagner et al., 2013). Apart from the target variable surface soil moisture, some products come with estimates of freeze/thaw state and vegetation optical depth, which are disentangled from the soil moisture impacts on the measured microwave signal during the retrieval process.

As none of the currently active missions covers a period long enough to study climate change impacts, ESA's Climate Change Initiative (CCI) endorsed the combination of available soil moisture products from active and passive microwave sensors into a consistent multi-decadal record. The ESA CCI soil moisture product currently combines soil moisture products from 11 different sensors into a homogenized daily product spanning the period 1978-2015 (Liu et al., 2012, 2011; Dorigo et al., 2016). Several studies have demonstrated the value of ESA CCI soil moisture for assessing long-term interactions between soil moisture and vegetation productivity (Barichivich et al., 2014; Chen et al., 2014; Dorigo et al., 2012; Muñoz et al., 2014).

Key to a proper assimilation of remotely sensed soil moisture into carbon models is a correct characterization of its errors. Apart from instrument errors which are common to all observations, the quality of microwave-based soil moisture retrievals is particularly impacted by vegetation cover, soil frost, snow cover, open water, topography, surface roughness, urban structures, and radio frequency interference (Dorigo et al., 2010; Kerr et al., 2012). Observations where a strong adverse impact of these factors is detected are usually masked during processing, which may lead to data gaps for

certain areas or periods of the year (Dorigo et al., 2015). If cases where their impact on the soil
635 moisture retrieval is only moderate, the errors that they introduce are either simulated during the
retrieval itself using error propagation methods, or assessed a posteriori against reference data using
various statistical methods (Draper et al., 2013).

    While the ASCAT and AMSR2 products come with an estimate of the error variance for each ob-
servation by error propagation (Naeimi et al., 2009; Parinussa et al., 2011) this is still not common
640 practice for all soil moisture products. Yet, no error propagation model perfectly represents all error
sources and interactions (Draper et al., 2013). On the other hand, the use of in-situ soil moisture
measurements to estimate random errors is hampered by their heterogeneous nature and large spatial
representativeness errors (Gruber et al., 2013). As an alternative, in recent years triple collocation
analysis (TCA) has firmly established itself as a robust alternative to estimate random errors in soil
645 moisture datasets without the need of an absolute 'true' reference (Dorigo et al., 2010; Scipal et al.,
2008). TCA estimates the error variances of three spatially and temporally collocated soil moisture
datasets with independent error structures, e.g. a radiometer-based, a scatterometer-based, and a land
surface model soil moisture dataset. Recently, the TCA has been intensively elaborated, e.g. to solve
for collinearities between errors (Gruber et al., 2016b) and non-linear dependencies between datasets
650 (Zwieback et al., 2016). The most remarkable advancement has been to express TCA-based error es-
timates as a signal-to-noise ratio, which facilitates a direct intercomparison of the skill of datasets in-
dependent of their dynamic ranges (Gruber et al., 2016a), 5. Although the TCA provides an estimate
that is entirely independent of any retrieval model assumptions, it only provides a single average er-
ror estimate for the entire period under consideration. Thus, synergistic use of error propagation and
655 triple collocation estimates shall be exploited to better capture the temporal error dynamics needed
for an optimal assimilation into carbon models. Due to the recent progress in product quality, er-
ror characterization, and operationalization, satellite-based soil moisture products have reached the
level of maturity that allows for a systematic assimilation into land surface models to improve the
models' hydrology. For example, Martens et al. (2016) showed that the assimilation of SMOS and
660 ESA CCI soil moisture generally has a small positive impact on soil water storages and evaporative
fluxes as simulated by the GLEAM land evaporation model. Surface soil moisture from ASCAT
is assimilated operationally in near-real-time into ECMWF Land Data Assimilation System to ob-
tain root-zone soil moisture (Albergel et al., 2012). Global root-zone soil moisture products based
on SMOS and SMAP are derived by a slightly different approach, which assimilate the observed
665 brightness temperatures instead of the retrieved surface soil moisture products (Lannoy and Reichle,
2016). The assimilation of satellite-based soil moisture products in terrestrial carbon cycle models
has been described above.

3.3.5 Biomass

Continental-scale biomass maps have been produced from space using both radar and lidar; these
670 rely on the returns from transmitted power, so are known as active sensors. Biomass here refers to
above-ground biomass (AGB), since there are no methods to measure the below-ground component,
and this is typically inferred from AGB using allometric equations. Furthermore, the emphasis is on
the AGB of forests, although a global dataset of AGB in all biomes for the period 1993-2012 has
been produced based on global passive microwave satellite data, hence with spatial resolution of 10
675 km or coarser (Liu et al., 2015).

Using long time series of C-band radar data provided by the ESA Envisat satellite, the growing
stock volume of northern hemisphere boreal and temperate forests has been estimated (Santoro et al.,
2011). Although available at 0.01° resolution, the accuracy of growing stock volume at this scale
is comparatively poor, and spatial averaging provides more reliable results: at 0.5° spacing, esti-
680 mated growing stock volume has a relative accuracy of 20-30% when tested against inventory data
(Santoro et al., 2013). Thurner et al. (2014) used this product to derive the carbon stock (above- and
below-ground) in boreal, temperate mixed and broadleaf, and temperate coniferous forests of forests
above 30° N (40.7, 24.5 and 14.5 PgC respectively). These values have estimated accuracies of
around 33-39% under a conservative approach to estimate uncertainty.

685 For tropical forests, the key sensor is the Geoscience Laser Altimeter System (GLAS) onboard
the Ice, Cloud and land Elevation Satellite (ICESat) which failed in 2009 (Lefsky, 2010). Its archive
of forest height estimates was the core dataset exploited to produce two pan-tropical biomass maps
(Saatchi et al., 2011; Baccini et al., 2012) at grid scales of 1 km and 500 m respectively; Saatchi et al.
(2011) also provide a map of the errors associated with the biomass estimates at each pixel. This is
690 produced by combining measurement errors, allometry errors, sampling errors, and prediction errors,
which are treated as independent and spatially uncorrelated. Further details are given in the supple-
mentary material to Saatchi et al. (2011). In an attempt to resolve differences between these two
maps, Avitabile et al. (2016) used an independent reference dataset of field observations to remove
the biases in the maps and then combined them to estimate the AGB in the tropical belt (23.4° S to
695 23.4° N). Testing against a reference dataset not used in the fusion process indicated that the fused
map had a RMSE 15-21% lower than that of the input maps and nearly unbiased estimates.

However, there are unresolved questions about large-scale biomass patterns across the Amazon
inferred from in situ and satellite data. Biomass maps derived from satellite data in Saatchi et al.
(2011) and Baccini et al. (2012) differ significantly from each other and from biomass maps derived
700 from in situ plots distributed across Amazonia using kriging (Mitchard et al., 2014). Neither satel-
lite product exhibits the strong increase in biomass from southwestern to northeastern Amazonia
inferred from in situ data. Mitchard et al. (2014) attributed this to failure to account for gradients in
wood density and regionally varying tree height-diameter relations when estimating biomass from
the satellite data. Saatchi et al. (2015) reject this analysis and claim that the trends and patterns in

Biogeosciences
Discussions

EGU

Open Access

705 Mitchard et al. (2014) are erroneous and a consequence of inadequate sampling. Resolving this dis-
agreement is of fundamental importance since it raises basic questions about accuracy, uncertainty,
and representativeness for both in situ and satellite-derived biomass data.

The next 4-5 years will dramatically improve our global knowledge of biomass, with the launch
of three missions aimed at measuring forest structure and biomass. The ESA BIOMASS mission
710 (European Space Agency, 2012), to be launched in 2021, is a P-band radar that will provide near-
global measurements of forest biomass and height. Around the same time the NASA-ISRO SAR
mission (NISAR) based on an L-band sensor will be deployed, providing measurements of biomass
in lower biomass forests (up to 100 t ha^{-1}). These highly complementary missions will be further
complemented by the NASA Global Ecosystem Dynamics Investigation vegetation lidar to be placed
715 on the International Space Station around 2019; this aims to provide the first global, high-resolution
observations of the vertical structure of tropical and temperate forests, from which biomass may be
estimated.

4 Conclusions

In the context of carbon cycle data assimilation this paper reviews the requirements and summarises
720 the availability and characteristics of some selected observations with a special focus on remotely
sensed Earth observation data. The paper also briefly recapitulates the assimilation systems capable
of integrating these data, a more comprehensive description of the underlying formalism is given in
Rayner et al. (2016) while MacBean et al. (2016) discuss the implementation strategies for a mul-
tiple data assimilation system and its impacts on the results. To take maximum advantage of these
725 data streams in carbon cycle data assimilation studies it is of utmost importance to have the appro-
priate knowledge of the observational characteristics of the observational data, here with a focus
on atellite products. This includes an understanding of the observable and its representativeness in
order to develop the appropriate observation operator (see also Kaminski and Mathieu, 2016) but
also the structure of any biases, random errors and error covariances (that is both the diagonal and
730 off-diagonal elements quantifying the correlations between different observations).

The benefit of using multiple data streams in a CCDAS lies in the complementarity of the data,
and thus in the ability to constrain different components of the underlying process model. For ex-
ample, while FAPAR data constrain mainly the phenology component of a terrestrial carbon cycle
model, soil moisture data, in contrast, constrain the hydrological component, but both components
735 are important elements of the model and determine the simulated carbon fluxes. In fact, because of
the model internal interactions and feedbacks among the components the simultaneous assimilation
of complementary observations has synergistic effects such that the constraint is larger than the sum
of the individual constraints as shown for instance by Kato et al. (2013) assimilating observations of
FAPAR and latent heat flux.

740   As a final remark one important aspect of observational data is their continuity since much of the important information is contained in response to climate anomalies. Fortunately, the set up of operational observeing systems such as ICOS for in-situ data or Copernicus for satellite data has created the necessary infrastructure to ensure such a long-term perspective in the provision of Earth observations.

Biogeosciences Open Access
Discussions
EGU

745   **Appendix A: List of Acronyms**

ACE-FTS	Atmospheric Chemistry Experiment - Fourier Transform Spectrometer
AGB	Above Ground Biomass
AIRS	Atmospheric Infrared Sounder
AMSR2	Advanced Microwave Scanning Radiometer 2
AMSR-E	Advanced Microwave Scanning Radiometer - Earth Observing System
ASCAT	Advanced Scatterometer
ATSR	Along Track Scanning Radiometers
AVHRR	Advanced Very High Resolution Radiometer
CCDAS	Carbon Cycle Data Assimilation System
CCI	Climate Change Initiative
ECMWF	European Centre for Medium-Range Weather Forecasts
ECV	Essential Climate Variable
EO	Earth Observation (in this form generally understood as from space)
ESA	European Space Agency
FAPAR	Fraction of Absorbed Photosynthetically Active Radiation
FLEX	FLuorescence EXplorer
GCOM-W1	Global Change Observation Mission 1st-Water
GLAS	Geoscience Laser Altimeter System
GLEAM	Global Land Evaporation Amsterdam Model
GOME-2	Global Ozone Monitoring Experiment-2
GOSAT	Greenhouse Gases Observing Satellite
GPP	Gross Primary Productivity
IASI	Infrared Atmospheric Sounding Interferometer
ICOS	Integrated Carbon Observing System
ICESat	Ice, Cloud and land Elevation Satellite
ISRO	Indian Space Research Organisation
JAXA	Japan Aerospace Exploration Agency
JRC-TIP	Joint Research Centre – Two-stream Inversion Package
MERIS	Medium Resolution Imaging Spectrometer
MIPAS	Michelson Interferometer for Passive Atmospheric Sounding
MISR	Multiangle Imaging SpectroRadiometer
MODIS	Moderate Resolution Imaging Spectroradiometer
NASA	National Aeronautics and Space Administration
NDVI	Normalized Difference Vegetation Index
NIR	Near Infrared
Obs4Mips	Observations for Model Intercomparisons Project
OCO-2	Orbiting Carbon Observatory 2
OE	Optimal Estimation

PDF	Probability Density Function
SAR	Synthetic Aperture Radar
SCIAMACHY	Scanning Imaging Absorption Spectrometer for Atmospheric Chartography
SeaWiFS	Sea-viewing Wide Field-of-view Sensor
SEVIRI	Spinning Enhanced Visible and InfraRed Imager
SIF	Sun-Induced Fluorescence
SMAP	Soil Moisture Active Passive
SMOS	Soil Moisture Ocean Salinity
SWIR	Shortwave Infrared
TANSO-FTS	Thermal And Near infrared Sensor for carbon Observations - Fourier Transform Spectrometer
TCA	Triple Collocation Analysis
TCCON	Total Carbon Column Observing Network
TCOS	Terrestrial Carbon Observation System
TROPOMI	TROPOspheric Monitoring Instrument

References

Albergel, C., de Rosnay, P., Gruhier, C., Muñoz Sabater, J., Hasenauer, S., Isaksen, L., Kerr, Y., and Wagner, W.: Evaluation of remotely sensed and modelled soil moisture products using global ground-based in situ observations, Remote Sensing of Environment, 118, 215–226, doi:10.1016/j.rse.2011.11.017, 2012.

755 Alyaari, A., Wigneron, J. P., Ducharne, A., Kerr, Y., Wagner, W., De Lannoy, G., Reichle, R., Al Bitar, A., Dorigo, W., Richaume, P., and Mialon, A.: Global-scale comparison of passive (SMOS) and active (ASCAT) satellite-based microwave soil moisture retrievals with soil moisture simulations (MERRA-Land), Remote Sensing of Environment, 152, 614–626, doi:10.1016/j.rse.2014.07.013, 2015.

Avitabile, V., Herold, M., Heuvelink, G. B. M., Lewis, S. L., Phillips, O. L., Asner, G. P., Armston, J., Ashton,
760 P. S., Banin, L., Bayol, N., Berry, N. J., Boeckx, P., de Jong, B. H. J., DeVries, B., Girardin, C. A. J., Kearsley, E., Lindsell, J. A., Lopez-Gonzalez, G., Lucas, R., Malhi, Y., Morel, A., Mitchard, E. T. A., Nagy, L., Qie, L., Quinones, M. J., Ryan, C. M., Ferry, S. J. W., Sunderland, T., Laurin, G. V., Gatti, R. C., Valentini, R., Verbeeck, H., Wijaya, A., and Willcock, S.: An integrated pan-tropical biomass map using multiple reference datasets, Global Change Biology, 22, 1406–1420, doi:10.1111/gcb.13139, 2016.

765 Baccini, A., Goetz, S. J., Walker, W. S., Laporte, N. T., Sun, M., Sulla-Menashe, D., Hackler, J., Beck, P. S. A., Dubayah, R., Friedl, M. A., Samanta, S., and Houghton, R. A.: Estimated carbon dioxide emissions from tropical deforestation improved by carbon-density maps, Nature Climate Change, 2012.

Bacour, C., Peylin, P., MacBean, N., Rayner, P. J., Delage, F., Chevallier, F., Weiss, M., Demarty, J., Santaren, D., Baret, F., Berveiller, D., Dufrene, E., and Prunet, P.: Joint assimilation of eddy covariance flux measure-
770 ments and FAPAR products over temperate forests within a process-oriented biosphere model, Journal of Geophysical Research: Biogeosciences, 120, 1839–1857, doi:10.1002/2015JG002966, 2015.

Baldocchi, D., Falge, E., Gu, L., Olson, R., Hollinger, D., Running, S., Anthoni, P., Bernhofer, C., Davis, K., Evans, R., Fuentes, J., Goldstein, A., Katul, G., Law, B., Lee, X., Malhi, Y., Meyers, T., Munger, W., Oechel, W., Paw, K. T., Pilegaard, K., Schmid, H. P., Valentini, R., Verma, S., Vesala, T., Wilson, K., and Wofsy, S.:
775 FLUXNET: A New Tool to Study the Temporal and Spatial Variability of Ecosystem–Scale Carbon Dioxide, Water Vapor, and Energy Flux Densities, Bulletin of the American Meteorological Society, 82, 2415–2434, doi:10.1175/1520-0477, 2001.

Baret, F., Hagolle, O., Geiger, B., Bicheron, P., Miras, B., Huc, M., Berthelot, B., Nino, F., Weiss, M., Samain, O., Roujean, J. L., and Leroy, M.: LAI, fAPAR and fCover CYCLOPES global products derived from
780 VEGETATION: Part 1: Principles of the algorithm, Remote Sensing of Environment, 110, 275 – 286, doi:10.1016/j.rse.2007.02.018, 2007.

Barichivich, J., Briffa, K. R., Myneni, R., Van der Schrier, G., Dorigo, W., Tucker, C. J., Osborn, T., and Melvin, T.: Temperature and Snow-Mediated Moisture Controls of Summer Photosynthetic Activity in Northern Terrestrial Ecosystems between 1982 and 2011, Remote Sensing, 6, 1390–1431, doi:10.3390/rs6021390,
785 2014.

Barrett, D. J.: Steady state turnover time of carbon in the Australian terrestrial biosphere, Global Biogeochemical Cycles, 16, 55–1, 2002.

Bergamaschi, P., Houweling, S., Segers, A., Krol, M., Frankenberg, C., Scheepmaker, R. A., Dlugokencky, E., Wofsy, S. C., Kort, E. A., Sweeney, C., Schuck, T., Brenninkmeijer, C., Chen, H., Beck, V., and Gerbig, C.:
790 Atmospheric CH_4 in the first decade of the 21st century: Inverse modeling analysis using SCIAMACHY

satellite retrievals and NOAA surface measurements, Journal of Geophysical Research: Atmospheres, 118, 7350–7369, doi:10.1002/jgrd.50480, 2013.

Berger, M., Moreno, J., Johannessen, J. A., Levelt, P. F., and Hanssen, R. F.: ESA's sentinel missions in support of Earth system science, Remote Sensing of Environment, 120, 84 – 90, doi:http://dx.doi.org/10.1016/j.rse.2011.07.023, the Sentinel Missions - New Opportunities for Science, 2012.

Boesch, H., Baker, D., Connor, B., Crisp, D., and Miller, C.: Global Characterization of CO_2 Column Retrievals from Shortwave-Infrared Satellite Observations of the Orbiting Carbon Observatory-2 Mission, Remote Sensing, 3, 270, doi:10.3390/rs3020270, 2011.

Bontemps, S., Herold, M., Kooistra, L., van Groenestijn, A., Hartley, A., Arino, O., Moreau, I., and Defourny, P.: Revisiting land cover observation to address the needs of the climate modeling community, Biogeosciences, 9, 2145–2157, doi:10.5194/bg-9-2145-2012, 2012.

Boone, C. D., Nassar, R., Walker, K. A., Rochon, Y., McLeod, S. D., Rinsland, C. P., and Bernath, P. F.: Retrievals for the atmospheric chemistry experiment Fourier-transform spectrometer, Appl. Opt., 44, 7218–7231, doi:10.1364/AO.44.007218, 2005.

Bovensmann, H., Burrows, J. P., Buchwitz, M., Frerick, J., Noël, S., Rozanov, V. V., Chance, K. V., and Goede, A. P. H.: SCIAMACHY: Mission Objectives and Measurement Modes, Journal of the Atmospheric Sciences, 56, 127–150, doi:10.1175/1520-0469(1999)056<0127:SMOAMM>2.0.CO;2, 1999.

Braswell, B. H., Sacks, W. J., Linder, E., and Schimel, D. S.: Estimating diurnal to annual ecosystem parameters by synthesis of a carbon flux model with eddy covariance net ecosystem exchange observations, Global Change Biology, 11, 335–355, doi:10.1111/j.1365-2486.2005.00897.x, 2005.

Buchwitz, M. and Reuter, M.: Merged SCIAMACHY/ENVISAT and TANSO-FTS/GOSAT atmospheric column-average dry-air mole fraction of CO_2 (XCO2), Technical Note, Version 1, http://www.esa-ghg-cci.org/?q=webfm_send/319, 2016.

Buchwitz, M., Rozanov, V. V., and Burrows, J. P.: A near-infrared optimized DOAS method for the fast global retrieval of atmospheric CH_4, CO, CO_2, H_2O, and N_2O total column amounts from SCIAMACHY Envisat-1 nadir radiances, Journal of Geophysical Research: Atmospheres, 105, 15 231–15 245, doi:10.1029/2000JD900191, 2000.

Buchwitz, M., Reuter, M., Schneising, O., Boesch, H., Guerlet, S., Dils, B., Aben, I., Armante, R., Bergamaschi, P., Blumenstock, T., Bovensmann, H., Brunner, D., Buchmann, B., Burrows, J., Butz, A., Chédin, A., Chevallier, F., Crevoisier, C., Deutscher, N., Frankenberg, C., Hase, F., Hasekamp, O., Heymann, J., Kaminski, T., Laeng, A., Lichtenberg, G., Mazière, M. D., Noël, S., Notholt, J., Orphal, J., Popp, C., Parker, R., Scholze, M., Sussmann, R., Stiller, G., Warneke, T., Zehner, C., Bril, A., Crisp, D., Griffith, D., Kuze, A., O'Dell, C., Oshchepkov, S., Sherlock, V., Suto, H., Wennberg, P., Wunch, D., Yokota, T., and Yoshida, Y.: The Greenhouse Gas Climate Change Initiative (GHG-CCI): Comparison and quality assessment of near-surface-sensitive satellite-derived CO_2 and CH_4 global data sets, Remote Sensing of Environment, 162, 344 – 362, doi:10.1016/j.rse.2013.04.024, 2015.

Buchwitz, M., Dils, B., Boesch, H., Crevoisier, C., Detmers, D., Frankenberg, C., Hasekamp, O., Hewson, W., Laeng, A., Noël, S., Notholt, J., Parker, R., Reuter, M., and Schneising, O.: ESA Climate Change Initiative (CCI) Product Validation and Intercomparison Report (PVIR) for the Essential Climate Variable (ECV)

Greenhouse Gases (GHG) for data set Climate Research Data Package No. 3 (CRDP No. 3), Version 4.0, http://www.esa-ghg-cci.org/?q=webfm_send/300, 2016.

Burrows, J. P., Hölzle, E., Goede, A. P. H., Visser, H., and Fricke, W.: SCIAMACHY – scanning imaging absorption spectrometer for atmospheric chartography, Acta Astronautica, 35, 445 – 451, doi:10.1016/0094-5765(94)00278-T, 1995.

Butz, A., Hasekamp, O. P., Frankenberg, C., Vidot, J., and Aben, I.: CH_4 retrievals from space-based solar backscatter measurements: Performance evaluation against simulated aerosol and cirrus loaded scenes, Journal of Geophysical Research: Atmospheres, 115, doi:10.1029/2010JD014514, 2010.

Butz, A., Guerlet, S., Hasekamp, O., Schepers, D., Galli, A., Aben, I., Frankenberg, C., Hartmann, J.-M., Tran, H., Kuze, A., Keppel-Aleks, G., Toon, G., Wunch, D., Wennberg, P., Deutscher, N., Griffith, D., Macatangay, R., Messerschmidt, J., Notholt, J., and Warneke, T.: Toward accurate CO_2 and CH_4 observations from GOSAT, Geophysical Research Letters, 38, doi:10.1029/2011GL047888, 2011.

Butz, A., Galli, A., Hasekamp, O., Landgraf, J., Tol, P., and Aben, I.: TROPOMI aboard Sentinel-5 Precursor: Prospective performance of CH_4 retrievals for aerosol and cirrus loaded atmospheres, Remote Sensing of Environment, 120, 267 – 276, doi:10.1016/j.rse.2011.05.030, 2012.

Cadule, P., Friedlingstein, P., Bopp, L., Sitch, S., Jones, C. D., Ciais, P., Piao, S. L., and Peylin, P.: Benchmarking coupled climate-carbon models against long-term atmospheric CO_2 measurements, Global Biogeochemical Cycles, 24, doi:10.1029/2009GB003556, 2010.

Ceccherini, G., Gobron, N., and Robustelli, M.: Harmonization of Fraction of Absorbed Photosynthetically Active Radiation (FAPAR) from Sea-ViewingWide Field-of-View Sensor (SeaWiFS) and Medium Resolution Imaging Spectrometer Instrument (MERIS), Remote Sensing, 5, 3357, doi:10.3390/rs5073357, 2013.

Chen, T., de Jeu, R. A. M., Liu, Y. Y., van der Werf, G. R., and Dolman, A. J.: Using satellite based soil moisture to quantify the water driven variability in NDVI: A case study over mainland Australia, Remote Sensing of Environment, 140, 330–338, 2014.

Chevallier, F., Alexe, M., Bergamaschi, P., Brunner, D., Feng, L., Houweling, S., Kaminski, T., Knorr, W., van Leeuwen, T. T., Marshall, J., Palmer, P. I., Scholze, M., Sundström, A.-M., and Vossbeck, M.: ESA Climate Change Initiative (CCI) Climate Assessment Report (CAR) for Climate Research Data Package No. 3 (CRDP No. 3) of the Essential Climate Variable (ECV) Greenhouse Gases (GHG), Version 3, http://www.esa-ghgcci.org/?q=webfm_send/318, 2016.

Ciais, P., Sabine, C., Bala, G., Bopp, L., Brovkin, V., Canadell, J., Chhabra, A., DeFries, R., Galloway, J., Heimann, M., Jones, C., Le Quéré, C., Myneni, R., Piao, S., and Thornton, P.: Carbon and Other Biogeochemical Cycles, book section 6, p. 465–570, Cambridge University Press, Cambridge, United Kingdom and New York, NY, USA, doi:10.1017/CBO9781107415324.015, 2013.

Ciais, P., Dolman, A. J., Bombelli, A., Duren, R., Peregon, A., Rayner, P. J., Miller, C., Gobron, N., Kinderman, G., Marland, G., Gruber, N., Chevallier, F., Andres, R. J., Balsamo, G., Bopp, L., Bréon, F.-M., Broquet, G., Dargaville, R., Battin, T. J., Borges, A., Bovensmann, H., Buchwitz, M., Butler, J., Canadell, J. G., Cook, R. B., DeFries, R., Engelen, R., Gurney, K. R., Heinze, C., Heimann, M., Held, A., Henry, M., Law, B., Luyssaert, S., Miller, J., Moriyama, T., Moulin, C., Myneni, R. B., Nussli, C., Obersteiner, M., Ojima, D., Pan, Y., Paris, J.-D., Piao, S. L., Poulter, B., Plummer, S., Quegan, S., Raymond, P., Reichstein, M., Rivier, L., Sabine, C., Schimel, D., Tarasova, O., Valentini, R., Wang, R., van der Werf, G., Wickland, D., Williams,

M., and Zehner, C.: Current systematic carbon-cycle observations and the need for implementing a policy-relevant carbon observing system, Biogeosciences, 11, 3547–3602, doi:10.5194/bg-11-3547-2014, 2014.

Ciais, P., Crisp, D., Denier van der Gon, H., Engelen, R., Heimann, M., Janssens-Maenhout, G., Rayner, P., and Scholze, M.: Towards a European Operational Observing System to Monitor Fossil CO_2 emissions, Final Report from the expert group, European Commission, B-1049 Brussels, Belgium, http://www.copernicus.eu/sites/default/files/library/CO2_Report_22Oct2015.pdf, 2015.

Cihlar, J., Denning, S., Ahem, F., Arino, O., Belward, A., Bretherton, F., Cramer, W., Dedieu, G., Field, C., Francey, R., Gommes, R., Gosz, J., Hibbard, K., Igarashi, T., Kabat, P., Olson, D., Plummer, S., Rasool, I., Raupach, M., Scholes, R., Townshend, J., Valentini, R., and Wickland, D.: Initiative to quantify terrestrial carbon sources and sinks, Eos, Transactions American Geophysical Union, 83, 1–7, doi:10.1029/2002EO000002, 2002.

Cogan, A. J., Boesch, H., Parker, R. J., Feng, L., Palmer, P. I., Blavier, J.-F. L., Deutscher, N. M., Macatangay, R., Notholt, J., Roehl, C., Warneke, T., and Wunch, D.: Atmospheric carbon dioxide retrieved from the Greenhouse gases Observing SATellite (GOSAT): Comparison with ground-based TCCON observations and GEOS-Chem model calculations, Journal of Geophysical Research: Atmospheres, 117, n/a–n/a, doi:10.1029/2012JD018087, d21301, 2012.

Crevoisier, C., Chédin, A., Matsueda, H., Machida, T., Armante, R., and Scott, N. A.: First year of upper tropospheric integrated content of CO_2 from IASI hyperspectral infrared observations, Atmospheric Chemistry and Physics, 9, 4797–4810, doi:10.5194/acp-9-4797-2009, 2009a.

Crevoisier, C., Nobileau, D., Fiore, A. M., Armante, R., Chédin, A., and Scott, N. A.: Tropospheric methane in the tropics – first year from IASI hyperspectral infrared observations, Atmospheric Chemistry and Physics, 9, 6337–6350, doi:10.5194/acp-9-6337-2009, 2009b.

Crisp, D., Atlas, R., Breon, F.-M., Brown, L., Burrows, J., Ciais, P., Connor, B., Doney, S., Fung, I., Jacob, D., Miller, C., O'Brien, D., Pawson, S., Randerson, J., Rayner, P., Salawitch, R., Sander, S., Sen, B., Stephens, G., Tans, P., Toon, G., Wennberg, P., Wofsy, S., Yung, Y., Kuang, Z., Chudasama, B., Sprague, G., Weiss, B., Pollock, R., Kenyon, D., and Schroll, S.: The Orbiting Carbon Observatory (OCO) mission, Advances in Space Research, 34, 700 – 709, doi:http://dx.doi.org/10.1016/j.asr.2003.08.062, trace Constituents in the Troposphere and Lower Stratosphere, 2004.

Crisp, D., Fisher, B. M., O'Dell, C., Frankenberg, C., Basilio, R., Bösch, H., Brown, L. R., Castano, R., Connor, B., Deutscher, N. M., Eldering, A., Griffith, D., Gunson, M., Kuze, A., Mandrake, L., McDuffie, J., Messerschmidt, J., Miller, C. E., Morino, I., Natraj, V., Notholt, J., O'Brien, D. M., Oyafuso, F., Polonsky, I., Robinson, J., Salawitch, R., Sherlock, V., Smyth, M., Suto, H., Taylor, T. E., Thompson, D. R., Wennberg, P. O., Wunch, D., and Yung, Y. L.: The ACOS CO_2 retrieval algorithm – Part II: Global XCO2 data characterization, Atmospheric Measurement Techniques, 5, 687–707, doi:10.5194/amt-5-687-2012, 2012.

Daley, R.: Atmospheric data analysis, Cambridge University Press, Cambridge, UK, 1991.

De Jeu, R. and Dorigo, W.: On the importance of satellite observed soil moisture, International Journal of Applied Earth Observation and Geoinformation, 45, Part B, 107–109, doi:10.1016/j.jag.2015.10.007, 2016.

Deering, D., Rouse, J., Haas, R., and Schell, J.: Measuring forage production of grazing units from Landsat MSS data, Proc. 10th Int. Symp. Remote Sensing Environ., University of Michigan, Ann Arbor, U.S.A., 1975.

Dils, B., Buchwitz, M., Reuter, M., Schneising, O., Boesch, H., Parker, R., Guerlet, S., Aben, I., Blumenstock, T., Burrows, J. P., Butz, A., Deutscher, N. M., Frankenberg, C., Hase, F., Hasekamp, O. P., Heymann, J., De Mazière, M., Notholt, J., Sussmann, R., Warneke, T., Griffith, D., Sherlock, V., and Wunch, D.: The Greenhouse Gas Climate Change Initiative (GHG-CCI): comparative valida-
915   tion of GHG-CCI SCIAMACHY/ENVISAT and TANSO-FTS/GOSAT CO_2 and CH_4 retrieval algorithm products with measurements from the TCCON, Atmospheric Measurement Techniques, 7, 1723–1744, doi:10.5194/amt-7-1723-2014, 2014.

Disney, M., Muller, J.-P., Kharbouche, S., Kaminski, T., Voßbeck, M., Lewis, P., and Pinty, B.: A New Global fAPAR and LAI Dataset Derived from Optimal Albedo Estimates: Comparison with MODIS Products, Re-
920   mote Sensing, 8, 275, doi:10.3390/rs8040275, http://www.mdpi.com/2072-4292/8/4/275, 2016.

D'Odorico, P., Gonsamo, A., Pinty, B., Gobron, N., Coops, N., Mendez, E., and Schaepman, M. E.: Intercomparison of fraction of absorbed photosynthetically active radiation products derived from satellite data over Europe, Remote Sensing of Environment, 142, 141 – 154, doi:10.1016/j.rse.2013.12.005, 2014.

Dorigo, W., Zurita-Milla, R., de Wit, A., Brazile, J., Singh, R., and Schaepman, M.: A review on reflective
925   remote sensing and data assimilation techniques for enhanced agroecosystem modeling, International Journal of Applied Earth Observation and Geoinformation, 9, 165 – 193, doi:10.1016/j.jag.2006.05.003, 2007.

Dorigo, W., De Jeu, R., Chung, D., Parinussa, R., Liu, Y., Wagner, W., and Fernandez-Prieto, D.: Evaluating global trends (1988-2010) in homogenized remotely sensed surface soil moisture, Geophysical Research Letters, 39, L18 405, doi:10.1029/2012gl052988, 2012.

930   Dorigo, W., Xaver, A., Vreugdenhil, M., Gruber, A., Hegyiová, A., Sanchis-Dufau, A., Wagner, W., and Drusch, M.: Global automated quality control of in-situ soil moisture data from the International Soil Moisture Network, Vadose Zone Journal, 12, doi:10.2136/vzj2012.0097, 2013.

Dorigo, W., Wagner, W., Albergel, C., Albrecht, F., Balsamo, G., Brocca, L., Chung, D., Ertl, M., Forkel, M., Gruber, A., Haas, E., Hamer, P., Hirschi, M., Ikonen, J., Jeu, R., Kidd, R., Lahoz, W., Liu, Y., Miralles,
935   D., Mistelbauer, T., Nicolai-Shaw, N., Parinussa, R., Pratola, C., Reimer, C., Schalie, R., Seneviratne, S., Smolander, T., and Lecomte, P.: ESA CCI Soil Moisture for improved Earth system understanding: state-of-the art and future directions, Remote Sensing of Environment, under review, 2016.

Dorigo, W. A., Scipal, K., Parinussa, R. M., Liu, Y. Y., Wagner, W., de Jeu, R. A. M., and Naeimi, V.: Error characterisation of global active and passive microwave soil moisture data sets, Hydrology and Earth System
940   Sciences, 14, 2605–2616, doi:10.5194/hess-14-2605-2010, 2010.

Dorigo, W. A., Wagner, W., Hohensinn, R., Hahn, S., Paulik, C., Xaver, A., Gruber, A., Drusch, M., Mecklenburg, S., van Oevelen, P., Robock, A., and Jackson, T.: The International Soil Moisture Network: a data hosting facility for global in situ soil moisture measurements, Hydrology and Earth System Sciences, 15, 1675–1698, doi:10.5194/hess-15-1675-2011, 2011.

945   Dorigo, W. A., Gruber, A., De Jeu, R. A. M., Wagner, W., Stacke, T., Loew, A., Albergel, C., Brocca, L., Chung, D., Parinussa, R. M., and Kidd, R.: Evaluation of the ESA CCI soil moisture product using ground-based observations, Remote Sensing of Environment, 162, 380–395, doi:10.1016/j.rse.2014.07.023, 2015.

Draper, C., Reichle, R., de Jeu, R., Naeimi, V., Parinussa, R., and Wagner, W.: Estimating root mean square errors in remotely sensed soil moisture over continental scale domains, Remote Sensing of Environment,
950   137, 288–298, doi:10.1016/j.rse.2013.06.013, 2013.

Drusch, M. and FLEX Team: FLEX Report for Assessment, ESA SP-1330/2, ESA–ESTEC, Noordwijk (The Netherlands), 2015.

Entekhabi, D., Njoku, E. G., O'Neill, P. E., Kellogg, K. H., Crow, W. T., Edelstein, W. N., Entin, J. K., Goodman, S. D., Jackson, T. J., Johnson, J., Kimball, J., Piepmeier, J. R., Koster, R. D., Martin, N., McDonald, K. C.,

955   Moghaddam, M., Moran, S., Reichle, R., Shi, J. C., Spencer, M. W., Thurman, S. W., Tsang, L., and Van Zyl, J.: The soil moisture active passive (SMAP) mission, Proceedings of the IEEE, 98, 704–716, 2010.

Enting, I. G.: Inverse Problems in Atmospheric Constituent Transport, Cambridge University Press, Cambridge, 2002.

European Space Agency: Report for Mission Selection: Biomass, Science authors: Quegan, S, Le Toan

960   T., Chave, J., Dall, J., Perrera, A. Papathanassiou, K., Rocca, F., Saatchi, S., Scipal, K., Shugart, H., Ulander, L. and Williams, M.ESA SP 1324/1, European Space Agency, Noordwijk, the Netherlands., http://esamultimedia.esa.int/docs/EarthObservation/SP1324-1_BIOMASSr.pdf, 2012.

FLUXNET2015: FLUXNET2015 Dataset, available at: http://fluxnet.fluxdata.org/data/fluxnet2015-dataset/, 2015.

965   Foley, A. M., Dalmonech, D., Friend, A. D., Aires, F., Archibald, A. T., Bartlein, P., Bopp, L., Chappellaz, J., Cox, P., Edwards, N. R., Feulner, G., Friedlingstein, P., Harrison, S. P., Hopcroft, P. O., Jones, C. D., Kolassa, J., Levine, J. G., Prentice, I. C., Pyle, J., Vázquez Riveiros, N., Wolff, E. W., and Zaehle, S.: Evaluation of biospheric components in Earth system models using modern and palaeo-observations: the state-of-the-art, Biogeosciences, 10, 8305–8328, doi:10.5194/bg-10-8305-2013, 2013.

970   Foucher, P. Y., Chédin, A., Dufour, G., Capelle, V., Boone, C. D., and Bernath, P.: Technical Note: Feasibility of CO_2 profile retrieval from limb viewing solar occultation made by the ACE-FTS instrument, Atmospheric Chemistry and Physics, 9, 2873–2890, doi:10.5194/acp-9-2873-2009, 2009.

Fox, A., Williams, M., Richardson, A. D., Cameron, D., Gove, J. H., Quaife, T., Ricciuto, D., Reichstein, M., Tomelleri, E., Trudinger, C. M., and Wijk, M. T. V.: The {REFLEX} project: Comparing different algo-

975   rithms and implementations for the inversion of a terrestrial ecosystem model against eddy covariance data, Agricultural and Forest Meteorology, 149, 1597 – 1615, doi:10.1016/j.agrformet.2009.05.002, 2009.

Frankenberg, C., Aben, I., Bergamaschi, P., Dlugokencky, E. J., van Hees, R., Houweling, S., van der Meer, P., Snel, R., and Tol, P.: Global column-averaged methane mixing ratios from 2003 to 2009 as derived from SCIAMACHY: Trends and variability, Journal of Geophysical Research: Atmospheres, 116,

980   doi:10.1029/2010JD014849, d04302, 2011a.

Frankenberg, C., Butz, A., and Toon, G. C.: Disentangling chlorophyll fluorescence from atmospheric scattering effects in O2A-band spectra of reflected sun-light, Geophysical Research Letters, 38, doi:10.1029/2010GL045896, 2011b.

Frankenberg, C., Fisher, J. B., Worden, J., Badgley, G., Saatchi, S. S., Lee, J.-E., Toon, G. C., Butz,

985   A., Jung, M., Kuze, A., and Yokota, T.: New global observations of the terrestrial carbon cycle from GOSAT: Patterns of plant fluorescence with gross primary productivity, Geophysical Research Letters, 38, doi:10.1029/2011GL048738, 2011c.

Frankenberg, C., O'Dell, C., Berry, J., Guanter, L., Joiner, J., Köhler, P., Pollock, R., and Taylor, T. E.: Prospects for chlorophyll fluorescence remote sensing from the Orbiting Carbon Observatory-2, Remote Sensing of

990   Environment, 147, 1–12, 2014.

GCOS: Global Climate Observing System: Systematic Observation Requirements for Satellite-based Products for Climate, GCOS - 154, https://www.wmo.int/pages/prog/gcos/Publications/gcos-154.pdf, 2011.

Giglio, L., Randerson, J. T., and van der Werf, G. R.: Analysis of daily, monthly, and annual burned area using the fourth-generation global fire emissions database (GFED4), Journal of Geophysical Research: Biogeosciences, 118, 317–328, doi:10.1002/jgrg.20042, 2013.

Global Carbon Project: Science Framework and Implementation. Earth System Science Partnership (IGBP, IHDP, WCRP, DIVERSITAS), Report No. 1; Global Carbon Project Report No. 1, 69pp, Canberra, 2003.

Gobron, N. and Verstraete, M. M.: FAPAR, fraction of absorbed photosynthetically active radiation – Assessment of the status of the development of the standards for the terrestrial essential climate variables, Version 8, GTOS Secretariat, FAO, Italy, http://www.fao.org/gtos/doc/ECVs/T10/T10.pdf, 2009.

Gobron, N., Pinty, B., Aussedat, O., Chen, J. M., Cohen, W. B., Fensholt, R., Gond, V., Huemmrich, K. F., Lavergne, T., Mélin, F., Privette, J. L., Sandholt, I., Taberner, M., Turner, D. P., Verstraete, M. M., and Widlowski, J.-L.: Evaluation of fraction of absorbed photosynthetically active radiation products for different canopy radiation transfer regimes: Methodology and results using Joint Research Center products derived from SeaWiFS against ground-based estimations, Journal of Geophysical Research: Atmospheres, 111, doi:10.1029/2005JD006511, 2006.

Goel, N. S. and Qin, W.: Influences of canopy architecture on relationships between various vegetation indices and LAI and Fpar: A computer simulation, Remote Sensing Reviews, 10, 309–347, doi:10.1080/02757259409532252, 1994.

Gruber, A., Dorigo, W., Zwieback, S., Xaver, A., and Wagner, W.: Characterizing coarse-scale representativeness of in-situ soil moisture measurements from the International Soil Moisture Network, Vadose Zone Journal, 12, doi:10.2136/vzj2012.0170, 2013.

Gruber, A., Su, C., Zwieback, S., Crow, W. T., Wagner, W., and Dorigo, W.: Recent advances in (soil moisture) triple collocation analysis, International Journal of Applied Earth Observation and Geoinformation, 45, Part B, 200–211, 2016a.

Gruber, A., Su, C. H., Crow, W. T., Zwieback, S., Dorigo, W. A., and Wagner, W.: Estimating error cross-correlations in soil moisture data sets using extended collocation analysis, Journal of Geophysical Research: Atmospheres, 121, 1208–1219, doi:10.1002/2015JD024027, 2016b.

Guanter, L., Frankenberg, C., Dudhia, A., Lewis, P. E., Gómez-Dans, J., Kuze, A., Suto, H., and Grainger, R. G.: Retrieval and global assessment of terrestrial chlorophyll fluorescence from GOSAT space measurements, Remote Sensing of Environment, 121, 236–251, 2012.

Guanter, L., Aben, I., Tol, P., Krijger, J. M., Hollstein, A., Köhler, P., Damm, A., Joiner, J., Frankenberg, C., and Landgraf, J.: Potential of the TROPOspheric Monitoring Instrument (TROPOMI) onboard the Sentinel-5 Precursor for the monitoring of terrestrial chlorophyll fluorescence, Atmospheric Measurement Techniques, 8, 1337–1352, doi:10.5194/amt-8-1337-2015, 2015.

Guanter, L., Zhang, Y., Jung, M., Joiner, J., Voigt, M., Berry, J. A., Frankenberg, C., Huete, A. R., Zarco-Tejada, P., Lee, J.-E., Moran, M. S., Ponce-Campos, G., Beer, C., Camps-Valls, G., Buchmann, N., Gianelle, D., Klumpp, K., Cescatti, A., Baker, J. M., and Griffis, T. J.: Global and time-resolved monitoring of crop photosynthesis with chlorophyll fluorescence, Proceedings of the National Academy of Sciences, 111, E1327–E1333, 2014.

Heymann, J., Reuter, M., Hilker, M., Buchwitz, M., Schneising, O., Bovensmann, H., Burrows, J. P., Kuze, A., Suto, H., Deutscher, N. M., Dubey, M. K., Griffith, D. W. T., Hase, F., Kawakami, S., Kivi, R., Morino, I., Petri, C., Roehl, C., Schneider, M., Sherlock, V., Sussmann, R., Velazco, V. A., Warneke, T., and Wunch, D.: Consistent satellite XCO$_2$ retrievals from SCIAMACHY and GOSAT using the BESD algorithm, Atmospheric Measurement Techniques, 8, 2961–2980, doi:10.5194/amt-8-2961-2015, 2015.

Hollmann, R., Merchant, C. J., Saunders, R., Downy, C., Buchwitz, M., Cazenave, A., Chuvieco, E., Defourny, P., de Leeuw, G., Forsberg, R., Holzer-Popp, T., Paul, F., Sandven, S., Sathyendranath, S., van Roozendael, M., and Wagner, W.: The ESA Climate Change Initiative: Satellite Data Records for Essential Climate Variables, Bulletin of the American Meteorological Society, 94, 1541–1552, doi:10.1175/BAMS-D-11-00254.1, 2013.

Houweling, S., Baker, D., Basu, S., Boesch, H., Butz, A., Chevallier, F., Deng, F., Dlugokencky, E. J., Feng, L., Ganshin, A., Hasekamp, O., Jones, D., Maksyutov, S., Marshall, J., Oda, T., O'Dell, C. W., Oshchepkov, S., Palmer, P. I., Peylin, P., Poussi, Z., Reum, F., Takagi, H., Yoshida, Y., and Zhuravlev, R.: An intercomparison of inverse models for estimating sources and sinks of CO$_2$ using GOSAT measurements, Journal of Geophysical Research: Atmospheres, 120, 5253–5266, doi:10.1002/2014JD022962, 2014JD022962, 2015.

Huete, A.: A soil-adjusted vegetation index (SAVI), Remote Sensing of Environment, 25, 295 – 309, doi:10.1016/0034-4257(88)90106-X, 1988.

Jackson, T.: Measuring surface soil moisture using passive microwave remote sensing., Hydrological Processes, 7, 139–152, 1993.

Joiner, J., Yoshida, Y., Vasilkov, A. P., Yoshida, Y., Corp, L. A., and Middleton, E. M.: First observations of global and seasonal terrestrial chlorophyll fluorescence from space, Biogeosciences, 8, 637–651, doi:10.5194/bg-8-637-2011, 2011.

Joiner, J., Yoshida, Y., Vasilkov, A. P., Middleton, E. M., Campbell, P. K. E., Yoshida, Y., Kuze, A., and Corp, L. A.: Filling-in of near-infrared solar lines by terrestrial fluorescence and other geophysical effects: simulations and space-based observations from SCIAMACHY and GOSAT, Atmospheric Measurement Techniques, 5, 809–829, doi:10.5194/amt-5-809-2012, 2012.

Joiner, J., Guanter, L., Lindstrot, R., Voigt, M., Vasilkov, A. P., Middleton, E. M., Huemmrich, K. F., Yoshida, Y., and Frankenberg, C.: Global monitoring of terrestrial chlorophyll fluorescence from moderate-spectral-resolution near-infrared satellite measurements: methodology, simulations, and application to GOME-2, Atmospheric Measurement Techniques, 6, 2803–2823, 2013.

Joiner, J., Yoshida, Y., Guanter, L., and Middleton, E. M.: New methods for retrieval of chlorophyll red fluorescence from hyper-spectral satellite instruments: simulations and application to GOME-2 and SCIAMACHY, Atmospheric Measurement Techniques Discussions, 2016, 1–41, doi:10.5194/amt-2015-387, 2016.

Kaminski, T. and Mathieu, P.-P.: Reviews and Syntheses: Flying the Satellite into Your Model, Biogeosciences Discussions, 2016, 1–25, doi:10.5194/bg-2016-237, 2016.

Kaminski, T., Knorr, W., Rayner, P., and Heimann, M.: Assimilating Atmospheric data into a Terrestrial Biosphere Model: A case study of the seasonal cycle, Global Biogeochemical Cycles, 16, 14–1–14–16, http://www.agu.org/pubs/crossref/2002/2001GB001463.shtml, 2002.

Kaminski, T., Knorr, W., Scholze, M., Gobron, N., Pinty, B., Giering, R., and Mathieu, P.-P.: Consistent assimilation of MERIS FAPAR and atmospheric CO_2 into a terrestrial vegetation model and interactive mission benefit analysis, Biogeosciences, 9, 3173–3184, doi:10.5194/bg-9-3173-2012, 2012.

Kaminski, T., Knorr, W., Schürmann, G., Scholze, M., Rayner, P. J., Zaehle, S., Blessing, S., Dorigo, W., Gayler, V., Giering, R., Gobron, N., Grant, J. P., Heimann, M., Hooker-Stroud, A., Houweling, S., Kato, T., Kattge, J., Kelley, D., Kemp, S., Koffi, E. N., Köstler, C., Mathieu, P.-P., Pinty, B., Reick, C. H., Rödenbeck, C., Schnur, R., Scipal, K., Sebald, C., Stacke, T., van Scheltinga, A. T., Vossbeck, M., Widmann, H., and Ziehn, T.: The BETHY/JSBACH Carbon Cycle Data Assimilation System: experiences and challenges, Journal of Geophysical Research: Biogeosciences, 118, 1414–1426, doi:10.1002/jgrg.20118, 2013.

Kaminski, T., Pinty, B., Voßbeck, M., Gobron, N., and Robustelli, M.: Consistent EO Land Surface Products including Uncertainty Estimates, Biogeosciences Discussions, 2016, 2016a.

Kaminski, T., Scholze, M., Vossbeck, M., Knorr, W., Buchwitz, M., and Reuter, M.: Constraining a terrestrial biosphere model with remotely sensed atmospheric carbon dioxide, "Remote Sensing of Environment", submitted, 2016b.

Kato, T., Knorr, W., Scholze, M., Veenendaal, E., Kaminski, T., Kattge, J., and Gobron, N.: Simultaneous assimilation of satellite and eddy covariance data for improving terrestrial water and carbon simulations at a semi-arid woodland site in Botswana, Biogeosciences, 10, 789–802, doi:10.5194/bg-10-789-2013, 2013.

Kaufman, Y. J. and Tanre, D.: Atmospherically resistant vegetation index (ARVI) for EOS-MODIS, IEEE Transactions on Geoscience and Remote Sensing, 30, 261–270, doi:10.1109/36.134076, 1992.

Keenan, T. F., Davidson, E., Moffat, A. M., Munger, W., and Richardson, A. D.: Using model-data fusion to interpret past trends, and quantify uncertainties in future projections, of terrestrial ecosystem carbon cycling, Global Change Biology, 18, 2555–2569, doi:10.1111/j.1365-2486.2012.02684.x, 2012.

Kelley, D. I., Prentice, I. C., Harrison, S. P., Wang, H., Simard, M., Fisher, J. B., and Willis, K. O.: A comprehensive benchmarking system for evaluating global vegetation models, Biogeosciences, 10, 3313–3340, doi:10.5194/bg-10-3313-2013, 2013.

Kerr, Y. H., Waldteufel, P., Wigneron, J. P., Delwart, S., Cabot, F., Boutin, J., Escorihuela, M. J., Font, J., Reul, N., Gruhier, C., Juglea, S. E., Drinkwater, M. R., Hahne, A., Martin-Neira, M., and Mecklenburg, S.: The SMOS Mission: New Tool for Monitoring Key Elements ofthe Global Water Cycle, Proceedings of the IEEE, 98, 666–687, doi:10.1109/JPROC.2010.2043032, 2010.

Kerr, Y. H., Waldteufel, P., Richaume, P., Wigneron, J. P., Ferrazzoli, P., Mahmoodi, A., Bitar, A. A., Cabot, F., Gruhier, C., Juglea, S. E., Leroux, D., Mialon, A., and Delwart, S.: The SMOS Soil Moisture Retrieval Algorithm, IEEE Transactions on Geoscience and Remote Sensing, 50, 1384–1403, doi:10.1109/TGRS.2012.2184548, 2012.

Knorr, W. and Kattge, J.: Inversion of terrestrial biosphere model parameter values against eddy covariance measurements using Monte Carlo sampling, Global Change Biology, 11, 1333–1351, 2005.

Knorr, W., Kaminski, T., Scholze, M., Gobron, N., Pinty, B., Giering, R., and Mathieu, P.-P.: Carbon cycle data assimilation with a generic phenology model, Journal of Geophysical Research: Biogeosciences, 115, doi:10.1029/2009JG001119, g04017, 2010.

Köhler, P., Guanter, L., and Frankenberg, C.: Simplified Physically Based Retrieval of Sun-Induced Chlorophyll Fluorescence From GOSAT Data, Geoscience and Remote Sensing Letters, IEEE, 12, 1446–1450, doi:10.1109/LGRS.2015.2407051, 2015a.

Köhler, P., Guanter, L., and Joiner, J.: A linear method for the retrieval of sun-induced chlorophyll fluorescence from GOME-2 and SCIAMACHY data, Atmospheric Measurement Techniques, 8, 2589–2608, doi:10.5194/amt-8-2589-2015, 2015b.

Konings, A. G., Piles, M., Rötzer, K., McColl, K. A., Chan, S. K., and Entekhabi, D.: Vegetation optical depth and scattering albedo retrieval using time series of dual-polarized L-band radiometer observations, Remote Sensing of Environment, 172, 178 – 189, doi:10.1016/j.rse.2015.11.009, 2016.

Kulawik, S., Wunch, D., O'Dell, C., Frankenberg, C., Reuter, M., Oda, T., Chevallier, F., Sherlock, V., Buchwitz, M., Osterman, G., Miller, C. E., Wennberg, P. O., Griffith, D., Morino, I., Dubey, M. K., Deutscher, N. M., Notholt, J., Hase, F., Warneke, T., Sussmann, R., Robinson, J., Strong, K., Schneider, M., DeÂ Mazière, M., Shiomi, K., Feist, D. G., Iraci, L. T., and Wolf, J.: Consistent evaluation of ACOS-GOSAT, BESD-SCIAMACHY, CarbonTracker, and MACC through comparisons to TCCON, Atmospheric Measurement Techniques, 9, 683–709, doi:10.5194/amt-9-683-2016, 2016.

Kuppel, S., Peylin, P., Chevallier, F., Bacour, C., Maignan, F., and Richardson, A. D.: Constraining a global ecosystem model with multi-site eddy-covariance data, Biogeosciences, 9, 3757–3776, doi:10.5194/bg-9-3757-2012, 2012.

Kuze, A., Suto, H., Nakajima, M., and Hamazaki, T.: Thermal and near infrared sensor for carbon observation Fourier-transform spectrometer on the Greenhouse Gases Observing Satellite for greenhouse gases monitoring, Appl. Opt., 48, 6716–6733, doi:10.1364/AO.48.006716, 2009.

Kuze, A., Taylor, T. E., Kataoka, F., Bruegge, C. J., Crisp, D., Harada, M., Helmlinger, M., Inoue, M., Kawakami, S., Kikuchi, N., Mitomi, Y., Murooka, J., Naitoh, M., O'Brien, D. M., O'Dell, C. W., Ohyama, H., Pollock, H., Schwandner, F. M., Shiomi, K., Suto, H., Takeda, T., Tanaka, T., Urabe, T., Yokota, T., and Yoshida, Y.: Long-Term Vicarious Calibration of GOSAT Short-Wave Sensors: Techniques for Error Reduction and New Estimates of Radiometric Degradation Factors, IEEE Transactions on Geoscience and Remote Sensing, 52, 3991–4004, doi:10.1109/TGRS.2013.2278696, 2014.

Laeng, A., Plieninger, J., von Clarmann, T., Grabowski, U., Stiller, G., Eckert, E., Glatthor, N., Haenel, F., Kellmann, S., Kiefer, M., Linden, A., Lossow, S., Deaver, L., Engel, A., Hervig, M., Levin, I., McHugh, M., Noël, S., Toon, G., and Walker, K.: Validation of MIPAS IMK/IAA methane profiles, Atmospheric Measurement Techniques, 8, 5251–5261, doi:10.5194/amt-8-5251-2015, 2015.

Lannoy, G. J. M. D. and Reichle, R. H.: Global Assimilation of Multiangle and Multipolarization SMOS Brightness Temperature Observations into the GEOS-5 Catchment Land Surface Model for Soil Moisture Estimation, Journal of Hydrometeorology, 17, 669–691, doi:10.1175/JHM-D-15-0037.1, 2016.

Lasslop, G., Reichstein, M., Kattge, J., and Papale, D.: Influences of observation errors in eddy flux data on inverse model parameter estimation, Biogeosciences, 5, 1311–1324, doi:10.5194/bg-5-1311-2008, 2008.

Le Quéré, C., Moriarty, R., Andrew, R. M., Canadell, J. G., Sitch, S., Korsbakken, J. I., Friedlingstein, P., Peters, G. P., Andres, R. J., Boden, T. A., Houghton, R. A., House, J. I., Keeling, R. F., Tans, P., Arneth, A., Bakker, D. C. E., Barbero, L., Bopp, L., Chang, J., Chevallier, F., Chini, L. P., Ciais, P., Fader, M., Feely, R. A., Gkritzalis, T., Harris, I., Hauck, J., Ilyina, T., Jain, A. K., Kato, E., Kitidis, V., Klein Goldewijk, K., Koven,

C., Landschützer, P., Lauvset, S. K., Lefèvre, N., Lenton, A., Lima, I. D., Metzl, N., Millero, F., Munro, D. R., Murata, A., Nabel, J. E. M. S., Nakaoka, S., Nojiri, Y., O'Brien, K., Olsen, A., Ono, T., Pérez, F. F., Pfeil, B., Pierrot, D., Poulter, B., Rehder, G., Rödenbeck, C., Saito, S., Schuster, U., Schwinger, J., Séférian, R., Steinhoff, T., Stocker, B. D., Sutton, A. J., Takahashi, T., Tilbrook, B., van der Laan-Luijkx, I. T., van der Werf, G. R., van Heuven, S., Vandemark, D., Viovy, N., Wiltshire, A., Zaehle, S., and Zeng, N.: Global Carbon Budget 2015, Earth System Science Data, 7, 349–396, doi:10.5194/essd-7-349-2015, 2015.

Lee, J.-E., Frankenberg, C., van der Tol, C., Berry, J. A., Guanter, L., Boyce, C. K., Fisher, J. B., Morrow, E., Worden, J. R., Asefi, S., Badgley, G., and Saatchi, S.: Forest productivity and water stress in Amazonia: observations from GOSAT chlorophyll fluorescence, Proceedings of the Royal Society B: Biological Sciences, 280, doi:10.1098/rspb.2013.0171, 2013.

Lefsky, M. A.: A global forest canopy height map from the Moderate Resolution Imaging Spectro-radiometer and the Geoscience Laser Altimeter System, Geophysical Research Letters, 37, n/a–n/a, doi:10.1029/2010GL043622, 2010.

Leprieur, C., Verstraete, M. M., and Pinty, B.: Evaluation of the performance of various vegetation indices to retrieve vegetation cover from AVHRR data, Remote Sensing Reviews, 10, 265–284, doi:10.1080/02757259409532250, 1994.

Li, Z.-L., Tang, B.-H., Wu, H., Ren, H., Yan, G., Wan, Z., Trigo, I. F., and Sobrino, J. A.: Satellite-derived land surface temperature: Current status and perspectives, Remote Sensing of Environment, 131, 14 – 37, doi:10.1016/j.rse.2012.12.008, 2013.

Liu, Q., Liang, S., Xiao, Z., and Fang, H.: Retrieval of leaf area index using temporal, spectral, and angular information from multiple satellite data, Remote Sensing of Environment, 145, 25 – 37, doi:10.1016/j.rse.2014.01.021, 2014.

Liu, Y., Parinussa, R., Dorigo, W., De Jeu, R., Wagner, W., Van Dijk, A. I. J. M., McCabe, M., and Evans, J.: Developing an improved soil moisture dataset by blending passive and active microwave satellite-based retrievals, Hydrology and Earth System Sciences, 15, 425–436, doi:10.5194/hess-15-425-2011, 2011.

Liu, Y., Dorigo, W., Parinussa, R., De Jeu, R., Wagner, W., McCabe, M., Evans, J., and Van Dijk, A. I. J. M.: Trend-preserving blending of passive and active microwave soil moisture retrievals, Remote Sensing of Environment, 123, 280–297, doi:10.1016/j.rse.2012.03.014, 2012.

Liu, Y. Y., van Dijk, A. I. J. M., de Jeu, R. A. M., Canadell, J. G., McCabe, M. F., Evans, J. P., and Wang, G.: Recent reversal in loss of global terrestrial biomass, Nature Climate Change, doi:10.1038/nclimate2581, 2015.

Luo, Y. Q., Randerson, J. T., Abramowitz, G., Bacour, C., Blyth, E., Carvalhais, N., Ciais, P., Dalmonech, D., Fisher, J. B., Fisher, R., Friedlingstein, P., Hibbard, K., Hoffman, F., Huntzinger, D., Jones, C. D., Koven, C., Lawrence, D., Li, D. J., Mahecha, M., Niu, S. L., Norby, R., Piao, S. L., Qi, X., Peylin, P., Prentice, I. C., Riley, W., Reichstein, M., Schwalm, C., Wang, Y. P., Xia, J. Y., Zaehle, S., and Zhou, X. H.: A framework for benchmarking land models, Biogeosciences, 9, 3857–3874, doi:10.5194/bg-9-3857-2012, 2012.

MacBean, N., Peylin, P., Chevallier, F., Scholze, M., and Schürmann, G.: Consistent assimilation of multiple data streams in a carbon cycle data assimilation system, Geoscientific Model Development, 9, 3569–3588, doi:10.5194/gmd-9-3569-2016, 2016.

Martens, B., Miralles, D., Lievens, H., Van der Schalie, R., De Jeu, R., Fernandez-Prieto, D., Beck, H. E., Dorigo, W., and Verhoest, N. E. C.: GLEAM v3.0: satellite-based land evaporation and root-zone soil moisture, Geoscientific Model Development Discussion, 2016.

Mathieu, P.-P. and O'Neill, A.: Data assimilation: From photon counts to Earth System forecasts, Remote Sensing of Environment, 112, 1258 – 1267, doi:10.1016/j.rse.2007.02.040, 2008.

Matthews, H. D., Eby, M., Ewen, T., Friedlingstein, P., and Hawkins, B. J.: What determines the magnitude of carbon cycle-climate feedbacks?, Global Biogeochemical Cycles, 21, 12 PP, doi:10.1029/2006GB002733, gB2012, 2007.

McCallum, I., Wagner, W., Schmullius, C., Shvidenko, A., Obersteiner, M., Fritz, S., and Nilsson, S.: Comparison of four global FAPAR datasets over Northern Eurasia for the year 2000, Remote Sensing of Environment, 114, 941 – 949, doi:10.1016/j.rse.2009.12.009, 2010.

Mitchard, E. T. A., Feldpausch, T. R., Brienen, R. J. W., Lopez-Gonzalez, G., Monteagudo, A., Baker, T. R., Lewis, S. L., Lloyd, J., Quesada, C. A., Gloor, M., ter Steege, H., Meir, P., Alvarez, E., Araujo-Murakami, A., Aragao, L. E. O. C., Arroyo, L., Aymard, G., Banki, O., Bonal, D., Brown, S., Brown, F. I., Ceron, C. E., Chama Moscoso, V., Chave, J., Comiskey, J. A., Cornejo, F., Corrales Medina, M., Da Costa, L., Costa, F. R. C., Di Fiore, A., Domingues, T. F., Erwin, T. L., Frederickson, T., Higuchi, N., Honorio Coronado, E. N., Killeen, T. J., Laurance, W. F., Levis, C., Magnusson, W. E., Marimon, B. S., Marimon Junior, B. H., Mendoza Polo, I., Mishra, P., Nascimento, M. T., Neill, D., Nunez Vargas, M. P., Palacios, W. A., Parada, A., Pardo Molina, G., Peña-Claros, M., Pitman, N., Peres, C. A., Poorter, L., Prieto, A., Ramirez-Angulo, H., Restrepo Correa, Z., Roopsind, A., Roucoux, K. H., Rudas, A., Salomao, R. P., Schietti, J., Silveira, M., de Souza, P. F., Steininger, M. K., Stropp, J., Terborgh, J., Thomas, R., Toledo, M., Torres-Lezama, A., van Andel, T. R., van der Heijden, G. M. F., Vieira, I. C. G., Vieira, S., Vilanova-Torre, E., Vos, V. A., Wang, O., Zartman, C. E., Malhi, Y., and Phillips, O. L.: Markedly divergent estimates of Amazon forest carbon density from ground plots and satellites, Global Ecology and Biogeography, 23, 935–946, doi:10.1111/geb.12168, 2014.

Moore, D. J., Hu, J., Sacks, W. J., Schimel, D. S., and Monson, R. K.: Estimating transpiration and the sensitivity of carbon uptake to water availability in a subalpine forest using a simple ecosystem process model informed by measured net CO_2 and H_2O fluxes, Agricultural and Forest Meteorology, 148, 1467 – 1477, doi:10.1016/j.agrformet.2008.04.013, 2008.

Muñoz, A. A., Barichivich, J., Christie, D. A., Dorigo, W., Sauchyn, D., González-Reyes, A., Villalba, R., Lara, A., Riquelme, N., and González, M. E.: Patterns and drivers of Araucaria araucana forest growth along a biophysical gradient in the northern Patagonian Andes: Linking tree rings with satellite observations of soil moisture, Austral Ecology, 39, 158–169, doi:10.1111/aec.12054, 2014.

Myneni, R., Hoffman, S., Knyazikhin, Y., Privette, J., Glassy, J., Tian, Y., Wang, Y., Song, X., Zhang, Y., Smith, G., Lotsch, A., Friedl, M., Morisette, J., Votava, P., Nemani, R., and Running, S.: Global products of vegetation leaf area and fraction absorbed {PAR} from year one of {MODIS} data, Remote Sensing of Environment, 83, 214 – 231, doi:10.1016/S0034-4257(02)00074-3, the Moderate Resolution Imaging Spectroradiometer (MODIS): a new generation of Land Surface Monitoring, 2002.

Naeimi, V., Scipal, K., Bartalis, Z., Hasenauer, S., and Wagner, W.: An Improved Soil Moisture Retrieval
   Algorithm for ERS and METOP Scatterometer Observations, IEEE Transactions on Geoscience and Remote
   Sensing, 47, 1999–2013, doi:10.1109/Tgrs.2009.2011617, 2009.

Noël, S., Bramstedt, K., Rozanov, A., Bovensmann, H., and Burrows, J. P.: Stratospheric methane profiles from
   SCIAMACHY solar occultation measurements derived with onion peeling DOAS, Atmospheric Measure-
   ment Techniques, 4, 2567–2577, doi:10.5194/amt-4-2567-2011, 2011.

Noël, S., Bramstedt, K., Hilker, M., Liebing, P., Plieninger, J., Reuter, M., Rozanov, A., Sioris, C. E., Bovens-
   mann, H., and Burrows, J. P.: Stratospheric CH_4 and CO_2 profiles derived from SCIAMACHY solar occul-
   tation measurements, Atmospheric Measurement Techniques, 9, 1485–1503, doi:10.5194/amt-9-1485-2016,
   2016.

Norton, A., Rayner, P. J., Scholze, M., and Koffi, E.: Global Gross Primary Productivity for 2015 inferred
   from OCO-2 SIF and a Carbon-Cycle Data Assimilation System, Abstract B53L-01 presented at 2016, Fall
   Meeting, AGU, San Francisco, CA, 12-16 December, 2016.

Ochsner, T., Cosh, M., Cuenca, R., Dorigo, W., Draper, C., Hagimoto, Y., Kerr, Y., Larson, K., Njoku, E., Small,
   E., and Zreda, M.: State of the art in large-scale soil moisture monitoring, Soil Science Society of America
   Journal, 77, 2013.

Owe, M., de Jeu, R., and Holmes, T.: Multisensor historical climatology of satellite-derived global land surface
   moisture, Journal of Geophysical Research-Earth Surface, 113, doi:10.1029/2007jf000769, 2008.

Parazoo, N. C., Bowman, K., Frankenberg, C., Lee, J.-E., Fisher, J. B., Worden, J., Jones, D. B. A., Berry,
   J., Collatz, G. J., Baker, I. T., Jung, M., Liu, J., Osterman, G., O'Dell, C., Sparks, A., Butz, A., Guerlet,
   S., Yoshida, Y., Chen, H., and Gerbig, C.: Interpreting seasonal changes in the carbon balance of southern
   Amazonia using measurements of XCO2 and chlorophyll fluorescence from GOSAT, Geophysical Research
   Letters, 40, 2829–2833, doi:10.1002/grl.50452, 2013.

Parinussa, R., Meesters, A., Liu, Y., Dorigo, W., Wagner, W., and De Jeu, R.: An analytical solution to estimate
   the error structure of a global soil moisture data set, IEEE Geoscience and Remote Sensing Letters, 8, 779–
   783, 2011.

Parker, R., Boesch, H., Cogan, A., Fraser, A., Feng, L., Palmer, P. I., Messerschmidt, J., Deutscher, N., Grif-
   fith, D. W. T., Notholt, J., Wennberg, P. O., and Wunch, D.: Methane observations from the Greenhouse
   Gases Observing SATellite: Comparison to ground-based TCCON data and model calculations, Geophysical
   Research Letters, 38, n/a–n/a, doi:10.1029/2011GL047871, l15807, 2011.

Peylin, P., Law, R. M., Gurney, K. R., Chevallier, F., Jacobson, A. R., Maki, T., Niwa, Y., Patra, P. K., Pe-
   ters, W., Rayner, P. J., Rödenbeck, C., van der Laan-Luijkx, I. T., and Zhang, X.: Global atmospheric
   carbon budget: results from an ensemble of atmospheric CO_2 inversions, Biogeosciences, 10, 6699–6720,
   doi:10.5194/bg-10-6699-2013, 2013.

Peylin, P., Bacour, C., MacBean, N., Leonard, S., Rayner, P. J., Kuppel, S., Koffi, E. N., Kane, A., Maignan,
   F., Chevallier, F., Ciais, P., and Prunet, P.: A new step-wise Carbon Cycle Data Assimilation System using
   multiple data streams to constrain the simulated land surface carbon cycle, Geoscientific Model Development
   Discussions, 2016, 1–52, doi:10.5194/gmd-2016-13, 2016.

Pickett-Heaps, C. A., Canadell, J. G., Briggs, P. R., Gobron, N., Haverd, V., Paget, M. J., Pinty, B., and
   Raupach, M. R.: Evaluation of six satellite-derived Fraction of Absorbed Photosynthetic Active Radia-

tion (FAPAR) products across the Australian continent, Remote Sensing of Environment, 140, 241 – 256, doi:10.1016/j.rse.2013.08.037, 2014.

Pinty, B. and Verstraete, M.: GEMI: A non-linear index to monitor global vegetation from satellites, Vegetatio, 101, 1335–1372, 1992.

Pinty, B., Leprieur, C., and Verstraete, M. M.: Towards a quantitative interpretation of vegetation indices Part 1: Biophysical canopy properties and classical indices, Remote Sensing Reviews, 7, 127–150, doi:10.1080/02757259309532171, 1993.

Pinty, B., Lavergne, T., Dickinson, R. E., Widlowski, J.-L., Gobron, N., and Verstraete, M. M.: Simplifying the Interaction of Land Surfaces with Radiation for Relating Remote Sensing Products to Climate Models, Journal of Geophysical Research – Atmospheres, 111, doi:10.1029/2005JD005952, 2006.

Pinty, B., Lavergne, T., Voßbeck, M., Kaminski, T., Aussedat, O., Giering, R., Gobron, N., Taberner, M., Verstraete, M. M., and Widlowski, J.-L.: Retrieving Surface Parameters for Climate Models from MODIS-MISR Albedo Products, Journal of Geophysical Research – Atmospheres, 112, 23– PP, doi:10.1029/2006JD008105, 2007.

Pinty, B., Lavergne, T., Kaminski, T., Aussedat, O., Giering, R., Gobron, N., Taberner, M., Verstraete, M. M., Voßbeck, M., and Widlowski, J.-L.: Partitioning the solar radiant fluxes in forest canopies in the presence of snow, Journal of Geophysical Research – Atmospheres, 113, 13– PP, doi:10.1029/2007JD009096, 2008.

Pinty, B., Andredakis, I., Clerici, M., Kaminski, T., Taberner, M., Verstraete, M. M., Gobron, N., Plummer, S., and Widlowski, J.-L.: Exploiting the MODIS albedos with the Two-stream Inversion Package (JRC-TIP): 1. Effective leaf area index, vegetation, and soil properties, Journal of Geophysical Research – Atmospheres, 116, D09 105, doi:10.1029/2010JD015372, 2011a.

Pinty, B., Clerici, M., Andredakis, I., Kaminski, T., Taberner, M., Verstraete, M. M., Gobron, N., Plummer, S., and Widlowski, J.-L.: Exploiting the MODIS albedos with the Two-stream Inversion Package (JRC-TIP): 2. Fractions of transmitted and absorbed fluxes in the vegetation and soil layers, Journal of Geophysical Research – Atmospheres, 116, D09 106, doi:10.1029/2010JD015373, 2011b.

Pinty, B., Clerici, M., Andredakis, I., Kaminski, T., Taberner, M., Verstraete, M. M., Gobron, N., Plummer, S., and Widlowski, J.-L.: Exploiting the MODIS albedos with the Two-stream Inversion Package (JRC-TIP): 2. Fractions of transmitted and absorbed fluxes in the vegetation and soil layers, Journal of Geophysical Research – Atmospheres, 116, doi:10.1029/2010JD015373, 2011c.

Porcar-Castell, A., Tyystjärvi, E., Atherton, J., van der Tol, C., Flexas, J., Pfündel, E. E., Moreno, J., Frankenberg, C., and Berry, J. A.: Linking chlorophyll$-a$ fluorescence to photosynthesis for remote sensing applications: mechanisms and challenges, Journal of Experimental Botany, doi:10.1093/jxb/eru191, 2014.

Prentice, I. C., Liang, X., Medlyn, B. E., and Wang, Y.-P.: Reliable, robust and realistic: the three R's of next-generation land-surface modelling, Atmospheric Chemistry and Physics, 15, 5987–6005, doi:10.5194/acp-15-5987-2015, 2015.

Raj, R., Hamm, N. A. S., Tol, C. V. D., and Stein, A.: Uncertainty analysis of gross primary production partitioned from net ecosystem exchange measurements, Biogeosciences, 13, 1409–1422, doi:10.5194/bg-13-1409-2016, 2016.

Randerson, J. T., Hoffman, F. M., Thornton, P. E., Mahowald, N. M., Lindsay, K., Lee, Y.-H., Nevison, C. D., Doney, S. C., Bonan, G., Stockli, R., Covey, C., Running, S. W., and Fung, I. Y.: Systematic assessment

of terrestrial biogeochemistry in coupled climate-carbon models, Global Change Biology, 15, 2462–2484,
1305   doi:10.1111/j.1365-2486.2009.01912.x, 2009.

Raoult, N. M., Jupp, T. E., Cox, P. M., and Luke, C. M.: Land surface parameter optimisation through
data assimilation: the adJULES system, Geoscientific Model Development Discussions, 2016, 1–26,
doi:10.5194/gmd-2015-281, 2016.

Raupach, M. R., Rayner, P. J., Barrett, D. J., DeFries, R. S., Heimann, M., Ojima, D. S., Quegan, S., and Schmul-
1310   lius, C. C.: Model-data synthesis in terrestrial carbon observation: methods, data requirements and data un-
certainty specifications, Global Change Biology, 11, 378–397, doi:10.1111/j.1365-2486.2005.00917.x, 2005.

Rayner, P., Scholze, M., Knorr, W., Kaminski, T., Giering, R., and Widmann, H.: Two decades of terrestrial
Carbon fluxes from a Carbon Cycle Data Assimilation System (CCDAS), Global Biogeochemical Cycles,
19, 20 PP, doi:10.1029/2004GB002254, 2005.

1315 Rayner, P., Michalak, A. M., and Chevallier, F.: Fundamentals of Data Assimilation, Geoscientific Model De-
velopment Discussions, 2016, 1–21, doi:10.5194/gmd-2016-148, 2016.

Reuter, M., Buchwitz, M., Schneising, O., Heymann, J., Bovensmann, H., and Burrows, J. P.: A method for
improved SCIAMACHY CO_2 retrieval in the presence of optically thin clouds, Atmospheric Measurement
Techniques, 3, 209–232, doi:10.5194/amt-3-209-2010, 2010.

1320 Reuter, M., Bovensmann, H., Buchwitz, M., Burrows, J. P., Connor, B. J., Deutscher, N. M., Griffith, D. W. T.,
Heymann, J., Keppel-Aleks, G., Messerschmidt, J., Notholt, J., Petri, C., Robinson, J., Schneising, O., Sher-
lock, V., Velazco, V., Warneke, T., Wennberg, P. O., and Wunch, D.: Retrieval of atmospheric CO_2 with en-
hanced accuracy and precision from SCIAMACHY: Validation with FTS measurements and comparison with
model results, Journal of Geophysical Research: Atmospheres, 116, n/a–n/a, doi:10.1029/2010JD015047,
1325   d04301, 2011.

Reuter, M., Bösch, H., Bovensmann, H., Bril, A., Buchwitz, M., Butz, A., Burrows, J. P., O'Dell, C. W., Guerlet,
S., Hasekamp, O., Heymann, J., Kikuchi, N., Oshchepkov, S., Parker, R., Pfeifer, S., Schneising, O., Yokota,
T., and Yoshida, Y.: A joint effort to deliver satellite retrieved atmospheric CO_2 concentrations for surface
flux inversions: the ensemble median algorithm EMMA, Atmospheric Chemistry and Physics, 13, 1771–
1330   1780, doi:10.5194/acp-13-1771-2013, 2013.

Reuter, M., Hilker, M., Schneising, O., Buchwitz, M., and Heymann, J.: ESA Climate Change Ini-
tiative (CCI) Comprehensive Error Characterisation Report: BESD full-physics retrieval algorithm
for XCO2 for the Essential Climate Variable (ECV) Greenhouse Gases (GHG), Version 2.0,
http://www.esa-ghg-cci.org/webfm_send/284, 2016.

1335 Ricciuto, D. M., Davis, K. J., and Keller, K.: A Bayesian calibration of a simple carbon cycle model:
The role of observations in estimating and reducing uncertainty, Global Biogeochemical Cycles, 22,
doi:10.1029/2006GB002908, gB2030, 2008.

Richardson, A. D., Williams, M., Hollinger, D. Y., Moore, D. J. P., Dail, D. B., Davidson, E. A., Scott, N. A.,
Evans, R. S., Hughes, H., Lee, J. T., Rodrigues, C., and Savage, K.: Estimating parameters of a forest
1340   ecosystem C model with measurements of stocks and fluxes as joint constraints, Oecologia, 164, 25–40,
doi:10.1007/s00442-010-1628-y, 2010.

Rogers, C. D.: Inverse Methods for Atmospheric Sounding: Theory and Practice, World Scientific Publishing,
2000.

Saatchi, S., Mascaro, J., Xu, L., Keller, M., Yang, Y., Duffy, P., Espirito-Santo, F., Baccini, A., Chambers,
1345   J., and Schimel, D.: Seeing the forest beyond the trees, Global Ecology and Biogeography, 24, 606–610,
doi:10.1111/geb.12256, 2015.

Saatchi, S. S., Harris, N. L., Brown, S., Lefsky, M., Mitchard, E. T. A., Salas, W., Zutta, B. R., Buermann, W.,
Lewis, S. L., Hagen, S., Petrova, S., White, L., Silman, M., and Morel, A.: Benchmark map of forest carbon
stocks in tropical regions across three continents, Proceedings of the National Academy of Sciences, 108,
1350   9899–9904, doi:10.1073/pnas.1019576108, 2011.

Santoro, M., Beer, C., Cartus, O., Schmullius, C., Shvidenko, A., McCallum, I., Wegmüller, U., and Wiesmann,
A.: Retrieval of growing stock volume in boreal forest using hyper-temporal series of Envisat ASA ScanSAR
backscatter measurements, Remote Sensing of Environment, 115, 490 – 507, doi:10.1016/j.rse.2010.09.018,
2011.

1355 Santoro, M., Cartus, O., Fransson, J. E., Shvidenko, A., McCallum, I., Hall, R. J., Beaudoin, A., Beer,
C., and Schmullius, C.: Estimates of Forest Growing Stock Volume for Sweden, Central Siberia, and
Quebec using Envisat Advanced Synthetic Aperture Radar Backscatter Data, Remote Sensing, 5, 4503,
doi:10.3390/rs5094503, 2013.

Schneising, O., Buchwitz, M., Burrows, J. P., Bovensmann, H., Reuter, M., Notholt, J., Macatangay,
1360   R., and Warneke, T.: Three years of greenhouse gas column-averaged dry air mole fractions re-
trieved from satellite â€“ Part 1: Carbon dioxide, Atmospheric Chemistry and Physics, 8, 3827–3853,
doi:10.5194/acp-8-3827-2008, 2008.

Schneising, O., Buchwitz, M., Burrows, J. P., Bovensmann, H., Bergamaschi, P., and Peters, W.: Three years
of greenhouse gas column-averaged dry air mole fractions retrieved from satellite â€“ Part 2: Methane,
1365   Atmospheric Chemistry and Physics, 9, 443–465, doi:10.5194/acp-9-443-2009, 2009.

Schneising, O., Buchwitz, M., Reuter, M., Heymann, J., Bovensmann, H., and Burrows, J. P.: Long-term anal-
ysis of carbon dioxide and methane column-averaged mole fractions retrieved from SCIAMACHY, Atmo-
spheric Chemistry and Physics, 11, 2863–2880, doi:10.5194/acp-11-2863-2011, 2011.

Schneising, O., Bergamaschi, P., Bovensmann, H., Buchwitz, M., Burrows, J. P., Deutscher, N. M., Griffith, D.
1370   W., Heymann, J., Macatangay, R., Messerschmidt, J., Notholt, J., Rettinger, M., Reuter, M., Sussmann, R.,
Velazco, V. A., Warneke, T., Wennberg, P. O., and Wunch, D.: Atmospheric greenhouse gases retrieved from
SCIAMACHY: comparison to ground-based FTS measurements and model results, Atmospheric Chemistry
and Physics, 12, 1527–1540, doi:10.5194/acp-12-1527-2012, 2012.

Scholze, M., Kaminski, T., Rayner, P., Knorr, W., and Giering, R.: Propagating uncertainty through prognostic
1375   CCDAS simulations, Journal of Geophysical Research, 112, doi:10.1029/2007JD008642, 2007.

Scholze, M., Allen, I., Bill Collins, B., Cornell, S., Huntingford, C., Joshi, M., Lowe, J., Smith, R., Ridgwell,
A., and Wild, O.: Understanding the Earth System - Global Change Science for Application, chap. 5 Earth
System Models: a tool to understand changes in the Earth System, Cambridge University Press, Cambridge,
UK, 2012.

1380 Scholze, M., Kaminski, T., Knorr, W., Blessing, S., Vossbeck, M., Grant, J., and Scipal, K.: Simultaneous
assimilation of {SMOS} soil moisture and atmospheric {CO2} in-situ observations to constrain the global
terrestrial carbon cycle, Remote Sensing of Environment, 180, 334 – 345, doi:10.1016/j.rse.2016.02.058,
special Issue: ESA's Soil Moisture and Ocean Salinity Mission - Achievements and Applications, 2016.

Schürmann, G. J., Kaminski, T., Köstler, C., Carvalhais, N., Voßbeck, M., Kattge, J., Giering, R., Rödenbeck,
1385   C., Heimann, M., and Zaehle, S.: Constraining a land surface model with multiple observations by application
        of the MPI-Carbon Cycle Data Assimilation System, Geoscientific Model Development Discussions, 2016,
        1–24, doi:10.5194/gmd-2015-263, 2016.

Scipal, K., Holmes, T., de Jeu, R., Naeimi, V., and Wagner, W.: A possible solution for the problem of
        estimating the error structure of global soil moisture data sets, Geophysical Research Letters, 35, –,
1390   doi:10.1029/2008gl035599, 2008.

Tao, X., Liang, S., and Wang, D.: Assessment of five global satellite products of fraction of absorbed photosyn-
        thetically active radiation: Intercomparison and direct validation against ground-based data, Remote Sensing
        of Environment, 163, 270 – 285, doi:10.1016/j.rse.2015.03.025, 2015.

Tarantola, A.: Inverse Problem Theory and methods for model parameter estimation, SIAM, Philadelphia, 2005.

1395   Thum, T., MacBean, N., Peylin, P., Bacour, C., Santaren, D., Longdoz, B., Loustau, D., and Ciais, P.: The po-
        tential benefit of using forest biomass data in addition to carbon and water fluxes measurements to constrain
        ecosystem model parameters: case studies at two temperate forest sites, Agricultural and Forest Meteorology,
        accepted, 2016.

Thurner, M., Beer, C., Santoro, M., Carvalhais, N., Wutzler, T., Schepaschenko, D., Shvidenko, A., Kompter,
1400   E., Ahrens, B., Levick, S. R., and Schmullius, C.: Carbon stock and density of northern boreal and temperate
        forests, Global Ecology and Biogeography, 23, 297–310, doi:10.1111/geb.12125, 2014.

Trudinger, C. M., Raupach, M. R., Rayner, P. J., Kattge, J., Liu, Q., Pak, B., Reichstein, M., Renzullo, L.,
        Richardson, A. D., Roxburgh, S. H., Styles, J., Wang, Y. P., Briggs, P., Barrett, D., and Nikolova, S.: OptIC
        project: An intercomparison of optimization techniques for parameter estimation in terrestrial biogeochem-
1405   ical models, Journal of Geophysical Research: Biogeosciences, 112, n/a–n/a, doi:10.1029/2006JG000367,
        g02027, 2007.

van der Molen, M. K., de Jeu, R. A. M., Wagner, W., van der Velde, I. R., Kolari, P., Kurbatova, J., Varlagin, A.,
        Maximov, T. C., Kononov, A. V., Ohta, T., Kotani, A., Krol, M. C., and Peters, W.: The effect of assimilating
        satellite-derived soil moisture data in SiBCASA on simulated carbon fluxes in Boreal Eurasia, Hydrol. Earth
1410   Syst. Sci., 20, 605–624, doi:10.5194/hess-20-605-2016, 2016.

Veefkind, J., Aben, I., McMullan, K., Förster, H., de Vries, J., Otter, G., Claas, J., Eskes, H., de Haan,
        J., Kleipool, Q., van Weele, M., Hasekamp, O., Hoogeveen, R., Landgraf, J., Snel, R., Tol, P., Ing-
        mann, P., Voors, R., Kruizinga, B., Vink, R., Visser, H., and Levelt, P.: {TROPOMI} on the {ESA}
        Sentinel-5 Precursor: A {GMES} mission for global observations of the atmospheric composition for
1415   climate, air quality and ozone layer applications, Remote Sensing of Environment, 120, 70 – 83,
        doi:http://dx.doi.org/10.1016/j.rse.2011.09.027, the Sentinel Missions - New Opportunities for Science,
        2012.

Wagner, W., Lemoine, G., and Rott, H.: A method for estimating soil moisture from ERS scatterometer and soil
        data, Remote Sensing of Environment, 70, 191–207, 1999.

1420   Wagner, W., Hahn, S., Kidd, R., Melzer, T., Bartalis, Z., Hasenauer, S., Figa-Saldaña, J., de Rosnay, P., Jann,
        A., Schneider, S., Komma, J., Kubu, G., Brugger, K., Aubrecht, C., Z´uger, J., Gangkofner, U., Kienberger,
        S., Brocca, L., Wang, Y., Bl´oschl, G., Eitzinger, J., and Steinnocher, K.: The ASCAT Soil Moisture Product:

A Review of its Specifications, Validation Results, and Emerging Applications, Meteorologische Zeitschrift, 22, 5–33, doi:10.1127/0941-2948/2013/0399, 2013.

1425 Walther, S., Voigt, M., Thum, T., Gonsamo, A., Zhang, Y., Koehler, P., Jung, M., Varlagin, A., and Guanter, L.: Satellite chlorophyll fluorescence measurements reveal large-scale decoupling of photosynthesis and greenness dynamics in boreal evergreen forests, Global Change Biology, doi:10.1111/gcb.13200, 2015.

Wang, Y. P., Leuning, R., Cleugh, H., and Coppin, P. A.: Parameter estimation in surface exchange models using non-linear inversion: How many parameters can w e estimate and which measurements are most useful?,

1430 Glob. Change Biol., 7, 495–510, 2001.

Widlowski, J.-L.: On the bias of instantaneous {FAPAR} estimates in open-canopy forests, Agricultural and Forest Meteorology, 150, 1501 – 1522, doi:j.agrformet.2010.07.011, 2010.

Williams, M., Schwarz, P. A., Law, B. E., Irvine, J., and Kurpius, M. R.: An improved analysis of forest carbon dynamics using data assimilation, Global Change Biology, 11, 89–105,

1435 doi:10.1111/j.1365-2486.2004.00891.x, 2005.

WMO: Greenhouse Gas Bulletin. The State of Greenhouse Gases in the Atmosphere Based on Global Observations through 2014., World Meteorological Organization, No. 11, 9 November, 2015.

Wolanin, A., Rozanov, V., Dinter, T., Noël, S., Vountas, M., Burrows, J., and Bracher, A.: Global retrieval of marine and terrestrial chlorophyll fluorescence at its red peak using hyperspectral top of atmosphere

1440 radiance measurements: Feasibility study and first results, Remote Sensing of Environment, 166, 243 – 261, doi:10.1016/j.rse.2015.05.018, 2015.

Wunch, D., Toon, G. C., Wennberg, P. O., Wofsy, S. C., Stephens, B. B., Fischer, M. L., Uchino, O., Abshire, J. B., Bernath, P., Biraud, S. C., Blavier, J.-F. L., Boone, C., Bowman, K. P., Browell, E. V., Campos, T., Connor, B. J., Daube, B. C., Deutscher, N. M., Diao, M., Elkins, J. W., Gerbig, C., Gottlieb, E., Griffith, D.

1445 W. T., Hurst, D. F., Jiménez, R., Keppel-Aleks, G., Kort, E. A., Macatangay, R., Machida, T., Matsueda, H., Moore, F., Morino, I., Park, S., Robinson, J., Roehl, C. M., Sawa, Y., Sherlock, V., Sweeney, C., Tanaka, T., and Zondlo, M. A.: Calibration of the Total Carbon Column Observing Network using aircraft profile data, Atmospheric Measurement Techniques, 3, 1351–1362, doi:10.5194/amt-3-1351-2010, 2010.

Wunch, D., Toon, G. C., Blavier, J.-F. L., Washenfelder, R. A., Notholt, J., Connor, B. J., Griffith, D. W. T.,

1450 Sherlock, V., and Wennberg, P. O.: The Total Carbon Column Observing Network, Philosophical Transactions of the Royal Society of London A: Mathematical, Physical and Engineering Sciences, 369, 2087–2112, doi:10.1098/rsta.2010.0240, 2011.

Xiong, X., Barnet, C., Maddy, E., Wofsy, S., Chen, L., Karion, A., and Sweeney, C.: Detection of methane depletion associated with stratospheric intrusion by atmospheric infrared sounder (AIRS), Geophysical Re-

1455 search Letters, 40, 2455–2459, doi:10.1002/grl.50476, 2013.

Yoshida, Y., Kikuchi, N., Morino, I., Uchino, O., Oshchepkov, S., Bril, A., Saeki, T., Schutgens, N., Toon, G. C., Wunch, D., Roehl, C. M., Wennberg, P. O., Griffith, D. W. T., Deutscher, N. M., Warneke, T., Notholt, J., Robinson, J., Sherlock, V., Connor, B., Rettinger, M., Sussmann, R., Ahonen, P., Heikkinen, P., Kyrö, E., Mendonca, J., Strong, K., Hase, F., Dohe, S., and Yokota, T.: Improvement of the retrieval algorithm

1460 for GOSAT SWIR XCO_2 and XCH_4 and their validation using TCCON data, Atmospheric Measurement Techniques, 6, 1533–1547, doi:10.5194/amt-6-1533-2013, 2013.
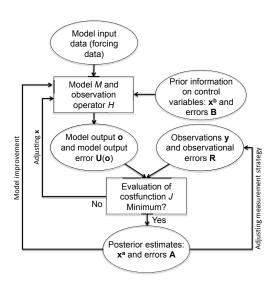
Zwieback, S., Su, C.-H., Gruber, A., Dorigo, W. A., and Wagner, W.: The Impact of Quadratic Nonlinear Re-
    lations between Soil Moisture Products on Uncertainty Estimates from Triple Collocation Analysis and Two
    Quadratic Extensions, Journal of Hydrometeorology, 17, 1725–1743, doi:doi:10.1175/JHM-D-15-0213.1,
1465   2016.

Figure 1. Schematic of a data assimilation system with **x** being the control vector containing the quantities to be updated by the assimilation. The inner loop ('Model-data comparison' box to 'Model and observation operator' box) indicates the assimilation process. Often, the analysis of residuals in model data comparison lead to either model improvements or adjustment of the measurement strategies (outer loops).
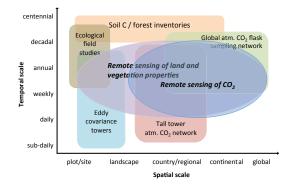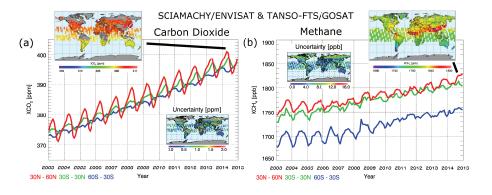

Figure 2. Space-time diagramme for a range of observations relevant for a Terrestrial Carbon Observation System.

Figure 3. Timeseries of satellite-derived XCO2 in 3 latitude bands (see annotation bottom left, e.g. red line: 30o-60oN) and maps showing the spatial distribution of XCO2 for April 2014 (top left map) and corresponding XCO2 uncertainty (bottom). (b) As (a) but for XCH4 (maps: September 2014).
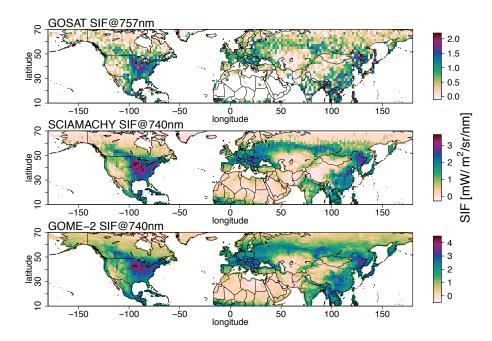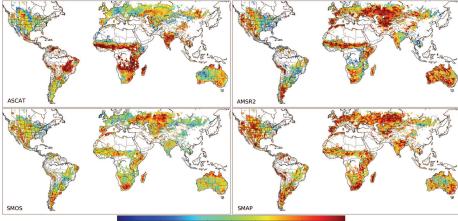

Figure 4. Maps of sun-induced fluorescence (SIF) for July 2010 derived from GOSAT, GOME-2 and SCIA-MACHY satellite data.

Figure 5. Signal-to-noise ratio (in dB), estimated with the Triple Collocation Analysis for four different satellite-based soil moisture products and a Land Surface Model. a) MetOp-A ASCAT based on the TU Wien method (Wagner et al., 1999); b) AMSR2 based on the LPRM model (Owe et al., 2008); c) SMOS L3 (Kerr et al., 2010); d) SMAP (Jackson, 1993). An SNR of -3 indicates a signal variance that is half of the noise variance, an SNR of 0 a signal variance equal to the noise variance, an SNR of 3 a signal variance that is twice the noise variance, and so on. In areas without data the TC could not be computed, e.g. because of too few observations in one of the datasets. For details see Gruber et al. (2016b).

Biogeosciences
Discussions

Open Access

EGU

Table 1. Overview SCIAMACHY/ENVISAT and TANSO-FTS/GOSAT XCO2 and XCH4 Level 2 data products (individual ground-pixel retrievals). For some products also Level 3, i.e. gridded data products are available (e.g. for CO2_SCI_WFMD and CH4_SCI_WFMD from http://www.iup.unibremen.de/sciamachy/NIR_NADIR_WFM_DOAS/ and merged SCIAMACHY and TANSO-FTS XCO2 and XCH4 products in Obs4MIPs format from http://www.esa-ghg-cci.org/)

Parameter	Sensor	Available at:
		Product (Reference)
XCO2	SCIAMACHY	http://www.esa-ghg-cci.org/
		CO2_SCI_BESD (Reuter et al., 2011)
		CH4_SCI_WFMD (Schneising et al., 2011)
	TANSO	http://www.gosat.nies.go.jp/en/
		NIES operational GOSAT (Yoshida et al., 2013)
		http://www.esa-ghg-cci.org/
		CO2_GOS_OCFP (Cogan et al., 2012)
		CO2_GOS_SRFP/RemoTeC (Butz et al., 2011)
		http://www.iup.uni-bremen.de/ heymann/besd_gosat.php
		GOSAT BESD (Heymann et al., 2015)
		http://disc.sci.gsfc.nasa.gov/acdisc/documentation/ACOS.html
		NASA ACOS (Crisp et al., 2012)
	SCIAMACHY &	http://www.esa-ghg-cci.org/
	TANSO merged	CO2_EMMA (Reuter et al., 2013)
	OCO-2	http://disc.sci.gsfc.nasa.gov/OCO-2
		NASA OCO-2 (Boesch et al., 2011)
XCH4	SCIAMACHY	http://www.esa-ghg-cci.org/
		CH4_SCI_WFMD (Schneising et al., 2011)
		CH4_SCI_IMAP (Frankenberg et al., 2011a)
	TANSO	http://www.gosat.nies.go.jp/en/
		NIES operational GOSAT (Yoshida et al., 2013)
		http://www.esa-ghg-cci.org/
		CH4_GOS_OCPR (Parker et al., 2011)
		CH4_GOS_SRPR/RemoTeC (Butz et al., 2010)
		CH4_GOS_OCFP (Parker et al., 2011)
		CH4_GOS_SRFP/RemoTeC (Butz et al., 2011)
	SCIAMCHY &	http://www.esa-ghg-cci.org/
	TANSO merged	CH4_EMMA (Reuter et al., 2013)

Table 2. Characteristics of a variety of FAPAR products, more details and products are provided by D'Odorico et al. (e.g. 2014); Pickett-Heaps et al. (e.g. 2014).

Name	Time period	Temporal resolution	Definition	Reference
MODIS	2000-present	8 days	Green canopy, direct radiation	Myneni et al. (2002)
SeaWiFS[1]	1997-2006	10 days	Green canopy, diffuse radiation	Gobron et al. (2006)
TIP-MODIS	2000-present	16 days	FAPAR/Green canopy, diffuse radiation	Pinty et al. (2011b)
TIP-GlobAlbedo	2002-2011	8 days	FAPAR/Green canopy, diffuse radiation	Disney et al. (2016)
Vegetation	1999-present	10 days	FAPAR, direct radiation	Baret et al. (2007)

1 The same algorithm is also used for MERIS, spanning a period form 2003-2012 with a 1 km, 10 day resolution.

Table 3. Selected characteristics of operating and planned spaceborne instruments able to deliver SIF data. Names of upcoming instruments are highlighted in italics. NIR stands for near-infrared. It must be noted that GOME-2 on MetOp-A has been operating with a reduced pixel size of $40 \times 40 \, km^2$ since July 2013.

	Time period	Overpass time	Spectral sampling	Global coverage	Spatial resolution	Temporal resolution
GOSAT	2009–today	Midday	NIR	No	10 km diam.	3 days
GOME-2	2007–today	Morning	red & NIR	Yes	$40 \times 80 \, km^2$	<2 days
SCIAMACHY	2003–2012	Morning	red & NIR	Yes	$30 \times 240 \, km^2$	<3 days
OCO-2	2014–today	Midday	NIR	No	$1.3 \times 2.3 \, km^2$	16 days
TROPOMI	~2017	Midday	red & NIR	Yes	$7 \times 7 \, km^2$	<1 day
FLEX	~2022	Morning	red & NIR	Yes	$0.3 \times 0.3 \, km^2$	<27 days

Table 4. Current (pre-)operational global soil moisture missions and products (for abbreviations / acronyms see List of Acronyms

Mission	Organisation	Measurement concept	Band	Mission start	Data access
MetOp - ASCAT	EUMETSAT	Real aperture radar (scatterometer)	C-band	Jan. 2007	http://hsaf.meteoam.it/soil-moisture.php http://land.copernicus.eu/global/products/swi
SMOS	ESA	Interferometric radiometer	L-band	Nov. 2009	http://www.catds.fr/
GCOM-W1 AMSR2	JAXA	Radiometer	C-band	May 2012	http://www.vandersat.com/ http://suzaku.eorc.jaxa.jp/GCOM_W/
SMAP	NASA	Radiometer & radar[1]	L-band	Jan. 2015	http://smap.jpl.nasa.gov/
Sentinel-1	ESA/ Copernicus	Synthetic aperture radar	C-band	Apr. 2014	https://www.eodc.eu/
CCI	ESA	Combined scatterometer and radiometer	L-, C-, X-Ku-band	Nov. 1978	http://www.esa-soilmoisture-cci.org

[1] SMAP's radar failed in July 2015